



# Kent Academic Repository

**Beirag, Nazar, Kumar, Chandan, Madan, Taruna, Shamji, Mohamed H., Bulla, Roberta, Mitchell, Daniel, Murugaiah, Valarmathy, Neto, Martin Mayora, Temperton, Nigel, Idicula-Thomas, Susan and others (2022) *Human surfactant protein D facilitates SARS-CoV-2 pseudotype binding and entry in DC-SIGN expressing cells, and downregulates spike protein induced inflammation.* *Frontiers in Immunology*, 13 .**

## Downloaded from

<https://kar.kent.ac.uk/95956/> The University of Kent's Academic Repository KAR

## The version of record is available from

<https://doi.org/10.3389/fimmu.2022.960733>

## This document version

Publisher pdf

## DOI for this version

<https://doi.org/10.3389/fimmu.2022.960733/full>

## Licence for this version

CC BY (Attribution)

## Additional information

## Versions of research works

### Versions of Record

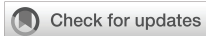
If this version is the version of record, it is the same as the published version available on the publisher's web site. Cite as the published version.

### Author Accepted Manuscripts

If this document is identified as the Author Accepted Manuscript it is the version after peer review but before type setting, copy editing or publisher branding. Cite as Surname, Initial. (Year) 'Title of article'. To be published in *Title of Journal*, Volume and issue numbers [peer-reviewed accepted version]. Available at: DOI or URL (Accessed: date).

## Enquiries

If you have questions about this document contact [ResearchSupport@kent.ac.uk](mailto:ResearchSupport@kent.ac.uk). Please include the URL of the record in KAR. If you believe that your, or a third party's rights have been compromised through this document please see our [Take Down policy](https://www.kent.ac.uk/guides/kar-the-kent-academic-repository#policies) (available from <https://www.kent.ac.uk/guides/kar-the-kent-academic-repository#policies>).



## OPEN ACCESS

## EDITED BY

Srinivasa Reddy Bonam,  
University of Texas Medical Branch at  
Galveston, United States

## REVIEWED BY

Sridhar Goud Nerella,  
National Institutes of Health (NIH),  
United States  
Ritwika Basu,  
University of Texas Medical Branch at  
Galveston, United States

## \*CORRESPONDENCE

Praveen M. Varghese  
praveenmathewsvarghese@gmail.com  
Uday Kishore  
ukishore@hotmail.com

<sup>†</sup>These authors have contributed  
equally to this work

## SPECIALTY SECTION

This article was submitted to  
Vaccines and Molecular Therapeutics,  
a section of the journal  
Frontiers in Immunology

RECEIVED 03 June 2022

ACCEPTED 28 June 2022

PUBLISHED 28 July 2022

## CITATION

Beirag N, Kumar C, Madan T,  
Shamji MH, Bulla R, Mitchell D,  
Murugaiah V, Neto MM, Temperton N,  
Idicula-Thomas S, Varghese PM and  
Kishore U (2022) Human surfactant  
protein D facilitates SARS-CoV-2  
pseudotype binding and entry in DC-  
SIGN expressing cells, and  
downregulates spike protein induced  
inflammation.  
*Front. Immunol.* 13:960733.  
doi: 10.3389/fimmu.2022.960733

## COPYRIGHT

© 2022 Beirag, Kumar, Madan, Shamji,  
Bulla, Mitchell, Murugaiah, Neto,  
Temperton, Idicula-Thomas, Varghese  
and Kishore. This is an open-access  
article distributed under the terms of  
the [Creative Commons Attribution  
License \(CC BY\)](https://creativecommons.org/licenses/by/4.0/). The use, distribution  
or reproduction in other forums is  
permitted, provided the original author  
(s) and the copyright owner(s) are  
credited and that the original  
publication in this journal is cited, in  
accordance with accepted academic  
practice. No use, distribution or  
reproduction is permitted which does  
not comply with these terms.

# Human surfactant protein D facilitates SARS-CoV-2 pseudotype binding and entry in DC-SIGN expressing cells, and downregulates spike protein induced inflammation

Nazar Beirag<sup>1†</sup>, Chandan Kumar<sup>2†</sup>, Taruna Madan<sup>3</sup>,  
Mohamed H. Shamji<sup>4</sup>, Roberta Bulla<sup>5</sup>, Daniel Mitchell<sup>6</sup>,  
Valarmathy Murugaiah<sup>1</sup>, Martin Mayora Neto<sup>7</sup>,  
Nigel Temperton<sup>7</sup>, Susan Idicula-Thomas<sup>2</sup>,  
Praveen M. Varghese<sup>1,8\*</sup> and Uday Kishore<sup>1,9\*</sup>

<sup>1</sup>Biosciences, College of Health, Medicine and Life Sciences, Brunel University London, Uxbridge, United Kingdom, <sup>2</sup>Biomedical Informatics Centre, National Institute for Research in Reproductive and Child Health, ICMR, Mumbai, Maharashtra, India, <sup>3</sup>Department of Innate Immunity, National Institute for Research in Reproductive and Child Health, ICMR, Mumbai, India, <sup>4</sup>Immunomodulation and Tolerance Group, Allergy and Clinical Immunology, Department of National Heart and Lung Institute and NIHR Biomedical Research Centre, Asthma UK Centre in Allergic Mechanisms of Asthma, Imperial College London, London, United Kingdom, <sup>5</sup>Department of Life Sciences, University of Trieste, Trieste, Italy, <sup>6</sup>WMS - Biomedical Sciences, Warwick Medical School, University of Warwick, Coventry, United Kingdom, <sup>7</sup>Viral Pseudotype Unit, Medway School of Pharmacy, University of Kent and Greenwich, United Kingdom, <sup>8</sup>School of Biosciences and Technology, Vellore Institute of Technology, Vellore, India, <sup>9</sup>Department of Veterinary Medicine, U.A.E. University, Al Ain, United Arab Emirates

Lung surfactant protein D (SP-D) and Dendritic cell-specific intercellular adhesion molecules-3 grabbing non-integrin (DC-SIGN) are pathogen recognising C-type lectin receptors. SP-D has a crucial immune function in detecting and clearing pulmonary pathogens; DC-SIGN is involved in facilitating dendritic cell interaction with naïve T cells to mount an anti-viral immune response. SP-D and DC-SIGN have been shown to interact with various viruses, including SARS-CoV-2, an enveloped RNA virus that causes COVID-19. A recombinant fragment of human SP-D (rfhSP-D) comprising of  $\alpha$ -helical neck region, carbohydrate recognition domain, and eight N-terminal Gly-X-Y repeats has been shown to bind SARS-CoV-2 Spike protein and inhibit SARS-CoV-2 replication by preventing viral entry in Vero cells and HEK293T cells expressing ACE2. DC-SIGN has also been shown to act as a cell surface receptor for SARS-CoV-2 independent of ACE2. Since rfhSP-D is known to interact with SARS-CoV-2 Spike protein and DC-SIGN, this study was aimed at investigating the potential of rfhSP-D in modulating SARS-CoV-2 infection. Coincubation of rfhSP-D with Spike protein improved the Spike Protein: DC-SIGN interaction. Molecular dynamic studies revealed that rfhSP-D stabilised the interaction between DC-SIGN and Spike protein. Cell binding analysis with

DC-SIGN expressing HEK 293T and THP-1 cells and rfhSP-D treated SARS-CoV-2 Spike pseudotypes confirmed the increased binding. Furthermore, infection assays using the pseudotypes revealed their increased uptake by DC-SIGN expressing cells. The immunomodulatory effect of rfhSP-D on the DC-SIGN: Spike protein interaction on DC-SIGN expressing epithelial and macrophage-like cell lines was also assessed by measuring the mRNA expression of cytokines and chemokines. RT-qPCR analysis showed that rfhSP-D treatment downregulated the mRNA expression levels of pro-inflammatory cytokines and chemokines such as TNF- $\alpha$ , IFN- $\alpha$ , IL-1 $\beta$ , IL-6, IL-8, and RANTES (as well as NF- $\kappa$ B) in DC-SIGN expressing cells challenged by Spike protein. Furthermore, rfhSP-D treatment was found to downregulate the mRNA levels of MHC class II in DC expressing THP-1 when compared to the untreated controls. We conclude that rfhSP-D helps stabilise the interaction between SARS-CoV-2 Spike protein and DC-SIGN and increases viral uptake by macrophages *via* DC-SIGN, suggesting an additional role for rfhSP-D in SARS-CoV-2 infection.

#### KEYWORDS

innate immune system, collectins, rfhSP-D, SARS-CoV-2, COVID-19, cytokine response

## Introduction

Pathogen recognition receptors (PRRs) are germline-encoded host sensors that detect pathogen-associated-molecular patterns (PAMPs) (1). PRRs play a vital part in the regular functioning of the innate immune system (2). They are expressed by innate immune cells, including dendritic cells (DCs), macrophages, neutrophils and monocytes (3). Toll-like receptors (TLRs) and C-type lectin receptors (CLRs) are key PRRs involved in host immunity against pathogens (4). Although CLRs are primarily expressed on myeloid cells such as DCs and macrophages, they vary between cell types, allowing specific immune response modifications upon target recognition (5). Receptors such as Dectin-2, Mincle, MGL (Macrophage galactose lectin), Langerin and DC-SIGN (Dendritic Cell-Specific Intercellular adhesion molecules-3-Grabbing Non-integrin) are CLRs that play a major role in the recognition of pathogenic fungi, bacteria, parasites, and viruses (6). The interaction of these CLRs with their ligands allows DCs to moderate the immune response towards either activation or tolerance, which is done through antigen presentation in lymphoid organs and the release of cytokines (7). DCs are responsible mainly for initiating antigen-specific immune responses. Therefore, they are localised at and patrol the sites of first contact with a pathogen, such as mucosal surfaces, including the pulmonary and nasopharyngeal mucosa. Likewise, alveolar macrophages are present in the lung alveoli (8).

DC-SIGN is a surface molecule on DCs that binds to the cell adhesion molecule ICAM-3 on T cells, enhancing DC-T cell

contact (9). DC-SIGN is a 44 kDa type II integral membrane protein with a single C-terminal CRD (carbohydrate recognition domain) supported by an  $\alpha$ -helical neck region with 7 and a half tandem repeats of a 23 amino-acid residue sequence (10, 11). A single transmembrane region anchors the protein, a cytoplasmic domain with recycling, internalisation, and intracellular signalling characteristics (11, 12). DC-SIGN forms oligomers on the cell surface, which improves the avidity of ligand binding and the specificity towards multiple repeated units that are likely to be related to the microbial surface features (13). Recently, DC-SIGN has been associated with promoting cis/trans infection of several viruses such as HIV, Cytomegalovirus, Dengue, Ebola and Zika (14–18). The ability of DCs to transmit HIV-1 to CD4<sup>+</sup> lymphocytes *via* DC-SIGN coupled with normal DC trafficking suggests that binding of the virus to DC-SIGN could be important in mucosal transmission of HIV-1 because DC-SIGN<sup>+</sup> DCs are present in the lamina propria at the mucosal surfaces (19). Recently, DC-SIGN has been reported to bind and enhance Severe acute respiratory syndrome coronavirus (SARS-CoV) and SARS-CoV-2 infection independent of ACE2 expression (20).

Another CLR molecule is human surfactant protein D (SP-D). SP-D belongs to the collectin family with a crucial role in pulmonary surfactant homeostasis and mucosal immunity. SP-D is primarily synthesised and secreted into the air space of the lungs by alveolar type II and Clara cells. Its primary structure is organised into four regions: a cysteine-rich N-terminus, a triple-helical collagen region, a neck region, and a C-terminal C-type

lectin or CRD. SP-D binds to glycosylated ligands on pathogens and initiates opsonisation, aggregation, and direct killing of microbes, facilitating their clearance by phagocytic cells such as macrophages. SP-D was also recently found to bind to the Spike protein of SARS-CoV-2, and inhibit viral replication in Caco-2 cells by promoting viral aggregation *in vitro* (21). A recombinant fragment of human SP-D (rfhSP-D), composed of homotrimer neck, CRD, and eight N-terminal Gly-X-Y regions, has been shown to have comparable immunological activities to native SP-D (22). It was shown to bind the HA protein of IAV and act as an entry inhibitor of IAV infection on A549 lung epithelial cells (23). Furthermore, rfhSP-D binds to gp120 and inhibits HIV-1 infectivity and replication in U937 monocytic cells, Jurkat T cells and PBMCs, inhibiting HIV-1 triggered cytokines storm (24). Importantly, rfhSP-D can directly bind to DC-SIGN. This interaction modulates HIV-1 capture and transfer to CD4<sup>+</sup> T cells (25). Recently, it has been shown rfhSP-D acts as an entry inhibitor of SARS-CoV-2 infection in Vero cells and HEK293T cells expressing ACE2 and TMPRSS2 (26, 27).

SARS-CoV-2, the causative pathogen of Coronavirus Disease 2019 (COVID-19), has resulted in around three million mortality worldwide (28, 29). The most common symptoms are fever, fatigue, and dry cough. The virus has been classified into Alpha, Beta, Gamma, Delta and Omicron variants based on mutations (30, 31). Some individuals can develop severe respiratory distress (32). SARS-CoV-2 is an enveloped RNA virus that uses a homotrimeric glycosylated spike (S) protein to interact with host cell receptors and promote fusion upon proteolytic activation (33). The transmembrane protease TMPRSS2 is known to mediate proteolytic cleavage at the S1/S2 and S2 domains. The receptor binding domain (RBD) is released by S1/S2 cleavage for high-affinity interaction with ACE2, whereas the S2 domain is released by S2 cleavage for effective virus fusion with the plasma membrane (23, 24). As a result, the virus is internalised by the host cells, resulting in viral replication. New copies of SARS-CoV 2 are internalised to infect more cells, increasing the viral load in the lungs, exacerbating the pro-inflammatory response, and extending the cellular and epithelial lung damage (34).

The sequence of events around the Spike protein/ACE2 interaction is well established; however, much remains to be unravelled about additional factors facilitating the infection, such as SARS-CoV-2 delivery to the ACE2 receptor (35). Indeed, Spike protein from both SARS-CoV and SARS-CoV-2 have similar affinity for ACE2 but show very different transmission rates (36, 37). The enhanced transmission rate of SARS-CoV-2 relative to SARS-CoV might result from an efficient viral adhesion through host-cell attachment factor, which may promote efficient infection of ACE2<sup>+</sup> cells (38, 39). In this framework, DC-SIGN bearing DCs and alveolar macrophages can play a role both in viral attachment and immune activation in the lungs (40–42).

Several studies have established the immune surveillance role of SP-D in terms of its ability to recognise viruses and modulate unwanted inflammatory responses (21, 25–27, 43–46). The interaction between SP-D and DC-SIGN during HIV-1 infection further provides an insight into the ability of SP-D to block DC-SIGN-mediated viral pathogenesis (25). In case of SARS-CoV-2, SP-D and rfhSP-D have been shown to bind to the S protein of the virus and inhibit viral infection and replication (21, 26, 27). Furthermore, DC-SIGN has also been reported to act as a facilitator and an entry receptor for SARS-CoV-2 infection, independent of ACE-2 expression (20, 47, 48). Thus, this study aimed to investigate the effects of rfhSP-D on DC-SIGN-mediated SARS-CoV-2 infection. Additionally, since DC-SIGN is highly expressed by DCs and macrophages, the study also explored the role of rfhSP-D on SARS-CoV-2 viral uptake by macrophage-like cells.

## Materials and methods

### Cell culture

HEK 293T cells were maintained in growth media, Dulbecco's Modified Eagle's Medium (DMEM) with Glutamax (Gibco) supplemented with 10% v/v foetal bovine serum (FBS), 100U/ml penicillin (Gibco), and 100µg/ml streptomycin (Gibco). The cells were cultured at 37°C in the presence of 5% v/v CO<sub>2</sub> until they were 70% confluent. HEK 293T cells were transiently transfected with a plasmid expressing human DC-SIGN (HG10200-UT; Sino Biological), using Promega FuGENE™ HD Transfection Reagent (Fisher Scientific). Next day, the cells were washed and cultured in the presence of hygromycin to select DC-SIGN expressing HEK-293T cells (DC HEK) (Thermo Fisher Scientific). Similarly, THP-1 cells were cultured in growth media. THP-1 cells were induced PMA to express DC-SIGN surface molecules (10 ng/mL) in combination with IL-4 (1000 units/mL) and incubated for 72 h (49).

### Expression and purification of a recombinant fragment of human SP-D (rfhSP-D) containing neck and CRD regions

A recombinant fragment of human SP-D (rfhSP-D) was expressed under bacteriophage T7 promoter in *Escherichia coli* BL21 (λDE3) pLysS (Invitrogen), transformed with plasmid containing cDNA sequences for neck, CRD regions and 8 Gly-X-Y repeats of human SP-D (26). Briefly, a primary inoculum of 25 ml bacterial culture was inoculated into 500 mL of Luria-Bertani (LB) broth containing 100 µg/ml ampicillin and 34 µg/ml chloramphenicol (Sigma-Aldrich), and grown to OD<sub>600</sub> of 0.6. The bacterial culture was then induced with 0.5 mM

isopropyl  $\beta$ -D-1-thiogalactopyranoside (IPTG) (Sigma-Aldrich) for 3 hours. The bacterial cell pellet was harvested and resuspended in lysis buffer [50 mM Tris-HCl pH 7.5, 200 mM NaCl, 5 mM EDTA pH 8, 0.1% Triton X-100, 0.1 mM phenyl-methyl-sulfonyl fluoride (PMSF), 50  $\mu$ g/ml lysozyme] and sonicated (ten cycles, 30 seconds each). The sonicate was centrifuged at 12000 x g for 30 minutes, followed by solubilisation of the pellet containing inclusion bodies in refolding buffer (50 mM Tris-HCl pH 7.5, 100 mM NaCl, 10 mM 2-Mercaptoethanol) containing 8M urea. The solubilised fraction was dialysed stepwise against refolding buffer containing 4M, 2M, 1M and 0M urea. The clear dialysate was loaded onto a maltose-agarose column (5ml; Sigma-Aldrich). The bound rfhSP-D was eluted using 50 mM Tris-HCl pH 7.5, 100 mM NaCl and 10 mM EDTA. The eluted fractions were then passed through a polymyxin B column in sodium deoxycholate buffer (Pierce<sup>TM</sup> High-Capacity Endotoxin Removal Spin Columns, Thermo Fisher) to remove endotoxin. The endotoxin levels were measured using ToxinSensor<sup>TM</sup> Chromogenic LAL Endotoxin Assay Kit (Genescript). The amount of endotoxin present in the rfhSP-D batches was ~4 pg/ $\mu$ g of rfhSP-D.

## Expression and purification of soluble tetrameric DC-SIGN

The pT5T construct expressing tetrameric form of human DC-SIGN was transformed into *Escherichia coli* BL21 ( $\lambda$ DE3). Protein expression was performed using bacterial culture in LB medium containing 50  $\mu$ g/ml ampicillin at 37°C until OD<sub>600</sub> reached 0.7. The bacteria culture was induced with 10 mM IPTG (Sigma -Aldrich) and incubated for 3 h at 37°C. Bacterial cells (1 L) were centrifuged at 4,500 x g for 15 min at 4°C. Next, the cell pellet was treated with 22 ml of lysis buffer containing 100 mM Tris-HCl pH 7.5, 0.5 mM NaCl, 2.5 mM EDTA pH 8, 0.5 mM PMSF, and 50  $\mu$ g/ml lysozyme, and left to stir for 1 h at 4°C. Cells were then sonicated for 10 cycles for 30 s with 2 min intervals. The sonicated suspension was spun at 10,000 g for 15 minutes at 4°C. The inclusion bodies present in the pellet were solubilised in 20 ml buffer containing 10 mM Tris-HCl, pH 7.0, 0.01%  $\beta$ -mercaptoethanol and 6 M urea by rotating on a shaker for 1 h at 4°C. The mixture was then centrifuged at 13,000 x g for 30 min at 4°C. The supernatant was drop-wise diluted fivefold with loading buffer containing 25 mM Tris-HCl pH 7.8, 1 M NaCl and 2.5mM CaCl<sub>2</sub> with gentle stirring. This was then dialysed against 2 L of loading buffer with three buffer changes every 3 h. Following further centrifugation at 13,000 x g for 15 min at 4°C, the supernatant was loaded onto a mannan-agarose column (5 ml; Sigma) pre-equilibrated with loading buffer. The column was washed with five-bed volumes of the loading buffer, and the bound protein was eluted in 1 ml fractions using the elution buffer containing 25 mM Tris-HCl pH 7.8, 1 M NaCl, and 2.5

mM EDTA. The absorbance was read at 280 nm, and the peak fractions were frozen at -20°C. The purity of the protein was analysed by 15% w/v SDS-PAGE.

## ELISA

Decreasing concentrations of recombinant DC-SIGN or rfhSP-D (2, 1, 0.5 or 0  $\mu$ g 100 $\mu$ l/well) were coated on polystyrene microtiter plates (Sigma-Aldrich) at 4°C overnight using carbonate/bicarbonate (CBC) buffer, pH 9.6 (Sigma-Aldrich). The microtiter wells were washed three times next day with PBST Buffer (PBS + 0.05% Tween 20) (Fisher Scientific). The wells were then blocked using 2% w/v BSA in PBS (Fisher Scientific) for 2 h at 37°C and washed three times using PBST. Constant concentration (2  $\mu$ g 100 $\mu$ l/well) of recombinant SARS-CoV-2 spike protein (RP-87680, Invitrogen) was added to the wells. After a 2-h incubation at 37°C, the wells were washed with PBST to eliminate any unbound protein. Polyclonal rabbit anti-SARS-CoV-2 spike (NR-52947, Bei-Resources) was used to probe the wells (1:5,000) in PBS and incubated for an additional 1 h at 37°C. Goat anti-rabbit IgG conjugated to horseradish peroxidase (HRP) (1:5,000) (Promega) was used to detect the bound protein. The colour was developed using 3,3',5,5'-tetramethylbenzidine (TMB) (Biolegend), and the reaction was stopped using 1M H<sub>2</sub>SO<sub>4</sub> (50  $\mu$ l/well; Sigma-Aldrich) and read at 450 nm spectrophotometrically.

For competitive ELISA, microtiter wells were coated overnight at 4°C with DC-SIGN protein (2  $\mu$ g; 100  $\mu$ l/well) and blocked. A fixed concentration of SARS-CoV-2 Spike protein (2 $\mu$ g; 100 $\mu$ l/well) and decreasing concentration (4.0, 2.0, 1.0, 0.5, 0  $\mu$ g; 100 $\mu$ l/well) of rfhSP-D in calcium buffer, was added to the well as competing proteins. The plate was incubated at 37°C for 1.5 h and then at 4°C for another 1.5 h. To remove any unbound protein, the wells were rinsed three times with PBST. Next, the wells were probed with polyclonal rabbit anti-SARS CoV-2 spike (1:5,000) in PBS and incubated for an additional 1 h at 37°C. The bound protein was detected using goat anti-rabbit IgG conjugated to HRP (1:5000), and the colour was developed using TMB (100  $\mu$ l/well). The reaction was stopped using 1M H<sub>2</sub>SO<sub>4</sub> (50  $\mu$ l/well; Sigma-Aldrich). The plate was read at 450 nm using a microplate reader (BioRad).

## Cell binding assay

SARS-CoV-2 spike pseudotypes were produced as previously described (44). Briefly, HEK 293T cells were cultured in growth media to 70-80% confluence at 37°C under 5% v/v CO<sub>2</sub>. Cells were co-transfected using FuGENE<sup>®</sup> HD Transfection Reagent (Promega) with Opti-MEM<sup>®</sup> diluted plasmids (450 ng of pCAGGS-SARS-CoV-2 spike, 500ng of

p8.91-lentiviral vector and 750 ng of pCSFLW). The transfected cells were incubated for 48h at 37°C under 5% v/v CO<sub>2</sub>. Post incubation, the medium containing the pseudotypes was harvested without disturbing the cell monolayer. The medium was then passed through a syringe driven 0.45 µm filter to remove any cell debris and the pseudotypes were harvested and stored at -80°C until further use.

DC-HEK and DC-THP-1 cells were seeded in microtiter wells separately in growth medium (1 x 10<sup>5</sup> cells/well) and incubated overnight at 37°C. The wells were washed three times with PBS, then rfhSP-D (20 µg/ml), pre-incubated with SARS-CoV-2 spike pseudotypes, were added to the corresponding wells and incubated at room temperature (RT) for 2 h. The microtiter wells were rinsed three times with PBS and fixed with 1% v/v paraformaldehyde (PFA) for 1 min at RT. The wells were washed again with PBS and incubated with polyclonal rabbit anti-SARS-CoV-2 spike (1:200 diluted in PBS) and incubated for 1 h at 37°C. After washing three times with PBST, the corresponding wells were probed with Alexa Fluor 488 conjugated goat anti-rabbit antibody (Abcam) diluted in PBS (1:200) for 1 h at RT. Readings were measured using a Clariostar Plus Microplate Reader (BMG Labtech).

## Fluorescence microscopy

DC-HEK cells were cultured on 13 mm glass coverslips to form a monolayer, followed by incubation with SARS-CoV-2 spike pseudotypes (50µl) at 37°C. For 30 min, cells were rinsed with PBS and fixed using 1% w/v PFA for 1 min. The cells were washed three times with PBS, then blocked with 5% w/v BSA in PBS (Fisher Scientific) for 30 minutes. The cells were incubated for 30-min with mouse anti-human DC-SIGN antibodies to detect DC-SIGN and rabbit anti-SARS-CoV-2 Spike antibodies. Next, cells were washed and incubated with a staining buffer containing Alexa Fluor 647 conjugated goat anti-mouse antibody (Abcam), Alexa fluor 488 conjugated goat anti-rabbit antibody (Abcam), and Hoechst (Invitrogen, Life Technologies). This incubation was done in the dark for 45 min. After rinsing with PBS, the mounted coverslips were visualised under a Leica DM4000 microscope.

## Luciferase reporter activity assay

SARS-CoV-2 spike pseudotypes, pre-incubated with rfhSP-D (20µg/ml), were added to DC-HEK and DC-THP-1 cells separately in a 96-well plate and incubated at 37°C for 24 h. The medium was removed, and cells were washed twice with PBS to remove any unbound SARS-CoV-2 spike pseudotypes and rfhSP-D. Fresh growth medium was added and incubated at 37°C for 48h. The cells were washed, and luciferase activity (RLU) was measured using ONE-Glo<sup>TM</sup> Luciferase Assay System

(Promega) and read on Clariostar Plus Microplate Reader (BMG Labtech).

## Quantitative qRT-PCR Analysis

DC-HEK and DC-THP-1 cells (0.5 X 10<sup>6</sup>) were seeded overnight in growth medium. Next day, SARS-CoV-2 Spike protein (500 ng/ml) was pre-incubated with rfhSP-D (20 µg/ml) for 2h at RT and added to DC-THP-1 cells in serum-free medium. Post incubation at 6h, 12h, 24h and 48h, the cells were washed with PBS gently and pelleted. GenElute Mammalian Total RNA Purification Kit (Sigma-Aldrich) was used to extract the total RNA. After RNA extraction, DNase I (Sigma-Aldrich) treatment was performed to remove any DNA contaminants, then the amount of RNA was quantified at A260 nm using a NanoDrop 2000/2000c (ThermoFisher). The purity of RNA was assessed using the ratio A260/A280. Two micrograms of total RNA were used to synthesize cDNA, using High-Capacity RNA to cDNA Kit (Applied Biosystems). The primer BLAST software (Basic Local Alignment Search Tool) was used to design primer sequences as listed in Table 1. qRT-PCR assay was performed using the Step One Plus system (Applied Biosciences). Each qPCR reaction was conducted in triplicates, containing 75 nM of forward and reverse primers, 5 µl Power SYBR Green Master Mix (Applied Biosystems), and 500 ng of cDNA. qPCR samples were run for 50°C, and 95°C for 2 and 10 min, followed by running the amplification template for 40 cycles, each cycle involving 15 s at 95°C and 1 min at 60°C. 18S rRNA was used as an endogenous control to normalise the gene expression.

## Molecular docking

Tripartite complex models of DC-SIGN tetramer, Spike trimer and rfhSP-D trimer were predicted through blind molecular docking using ZDOCK module of Discovery Studio 2021. The structural coordinates for DC-SIGN (CRD), spike and rfhSP-D were retrieved from PDB with IDs as 1K9I, 6XM3, and 1PW9, respectively. Docking was performed in two stages. In the first stage, DC-SIGN (CRD) tetramer was blind docked individually with rfhSP-D trimer (complex A) and spike trimer (complex B). The top ranked poses were analysed for intermolecular interactions and corroborated based on previous studies (25).

In the second stage, the selected docked pose of complex A was further blind docked with spike trimer to build a tripartite complex of DC-SIGN (CRD), Spike and rfhSP-D (complex C). The tripartite complex was selected based on the docking score and intermolecular interactions that were in agreement with reports (26).

TABLE 1 Forward and reverse primers used for RT-qPCR.

Target Primer	Forward Primer	Reverse Primer
18S	5'-ATGGCCGTTT TTAGTTGGTG-3'	5'-CGCTGAGCCA GTCAGTGTAG-3'
TNF- $\alpha$	5'-AGCCCATGTT GTAGCAAACC-3'	5'-TGAGGTACAG GCCCTCTGAT-3'
IL-6	5'-GAAAGCAGCA AAGAGGCACT-3	5'-TTTCACCAGG CAAGTCTCCT-3'
IL-8	5'-GGTGCAGTTTT GCCAAGGAG-3'	5'-CACCCAGTTTT CCTTGGGGT-3'
NF- $\kappa$ B	5'-GTATTTCAACCA CAGATGGCACT-3'	5'-AACCTTTGCTG GTCCACAT-3'
RANTES	5'-GCGGGTACCAT GAAGATCTCTG-3'	5'-GGGTCAGAATC AAGAAACCTC-3'
IFN- $\alpha$	5'-TTTCTCCTG CCTGAAGGACAG-3'	5'-GTCATGATTC TGCTCTGAC A-3'
IFN- $\beta$	5'-GGCTTTTCAGT CTGCATCG-3'	5'-TCTGTAC TCTCCTC TTTCCA-3
MHC II	5'-TAAGGCACATGGA GGTGATG-3'	5'-GTACGGAGC AATCGAAGAGG-3'

## Molecular dynamics (MD) simulation

MD simulations for the complexes B, C1 and C2 were performed using GROMACS v2020.6 (50). The force field AMBER99SB was applied with improved protein side-chain torsion potentials (51). All the three complexes were solvated in triclinic periodic box condition using TIP3P water molecules with a distance of 1.5 nm from the center of the complex. Complexes were neutralized by adding Na<sup>+</sup> counter ions and subsequently minimized for 5000 energy steps using steepest descent algorithm with a tolerance of 1000 kJ/mol/nm. Equilibration was performed using NVT and NPT ensembles for 50,000 steps. Finally, MD was run at constant temperature (300 K) and pressure (1 atm) for 20ns. The analyses of obtained MD trajectories were carried out using GROMACS utility tools.

## Statistical analysis

Graphs were generated using GraphPad Prism 8.0 software. The statistical significance was considered as indicated in the figure legends between treated and untreated conditions. Error bars show SD or SEM as stated in the figure legends.

## Results

### Both DC-SIGN and rhfSP-D bind to SARS-CoV 2 spike protein

An indirect ELISA was performed by coating microtiter plates with decreasing concentration of either rhfSP-D or DC-SIGN and probing with anti-SARS-CoV-2 spike antibody to confirm the protein-protein interaction between the two

proteins. Both DC-SIGN (Figure 1A) and rhfSP-D (Figure 1B) independently exhibited a dose-dependent increase in binding at all tested concentrations. Since both rhfSP-D and DC-SIGN bound SARS-CoV-2 Spike protein independently, a competitive ELISA was performed to evaluate if rhfSP-D would interfere with the binding between Spike protein and DC-SIGN. As a matter of fact, addition of rhfSP-D enhanced the binding of DC-SIGN to the Spike protein in a dose-dependent manner (Figure 1C).

### rhfSP-D treatment enhances DC-SIGN mediated binding and uptake of SARS-CoV-2 pseudotyped viral particles

Since rhfSP-D was found to interact with DC-SIGN and Spike protein, we evaluated the ability of rhfSP-D to mediate the binding of SARS-CoV-2 to DC-SIGN expressing cells. HEK 293T cells were transfected with a construct containing a DNA sequence of full-length human DC-SIGN to induce DC-SIGN cell surface expression. As previous studies have established the ability of SARS-CoV-2 spike protein to bind DC-SIGN, the binding of the SARS-CoV-2 spike protein-expressing pseudotypes to DC-HEK cells was also confirmed microscopically (Figure 2). To assess the effect of rhfSP-D on pseudotypes binding to DC HEK cells, the cells were challenged with rhfSP-D (20 $\mu$ g/ml) treated SARS-CoV-2 Spike protein-expressing pseudotype. Increased binding (~50%) in the treated samples (DC-HEK + SARS-CoV-2 spike Pseudotypes + rhfSP-D) compared to their untreated counterparts (DC-HEK + SARS-CoV-2 spike Pseudotypes) was observed (Figure 3A). The quantitative evaluation of the binding of the pseudotypes was also performed using THP-1 cells treated with PMA and IL-4 to induce the expression of native DC-SIGN. A similar result was

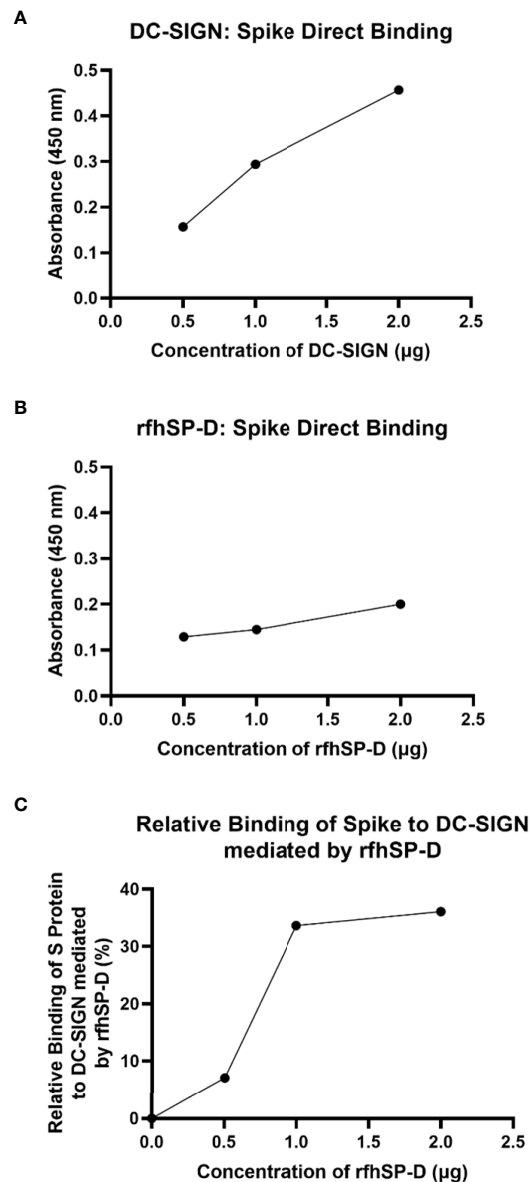


FIGURE 1

rfhSP-D promotes interaction between SARS-CoV-2 Spike protein and DC-SIGN. The binding of immobilised DC-SIGN (A) or immobilised rfhSP-D (B) to SARS-CoV-2 spike proteins was analysed by ELISA. Microtiter wells were coated with a decreasing concentration of DC-SIGN or rfhSP-D (2, 1, 0.5 or 0 µg per well) proteins and incubated with a constant amount of SARS-CoV-2 Spike protein (2 µg per well). Both proteins were found to bind Spike protein in a dose-dependent manner. Competitive ELISA (C) was performed to analyse the effect of rfhSP-D on DC-SIGN: Spike protein interaction. rfhSP-D brought about increased binding between Spike protein and DC-SIGN. Since increasing the concentration of rfhSP-D was found to increase the detectable amount of Spike protein, it seems to suggest the existence of distinct binding sites for the Spike protein on both C type lectins. The data were expressed as a mean of three independent experiments done in triplicates  $\pm$  SEM.

obtained using DC-SIGN expressing THP-1 macrophage-like cells. rfhSP-D treatment was found to increase the binding efficiency of the pseudotypes to the THP-1 cells expressing DC-SIGN by  $\sim$ 25%, compared to the untreated controls (Figure 3B).

To evaluate the impact of rfhSP-D on the transduction of pseudotypes to DC-HEK cells, the cells were treated with rfhSP-

D (20µg/ml) and challenged with SARS-CoV-2 Spike protein-expressing pseudotypes for 24h. Higher luciferase activity ( $\sim$ 190%) in the treated samples (DC-HEK + SARS-CoV-2 spike pseudotypes + rfhSP-D) as compared with their untreated counterparts (DC-HEK + SARS-CoV-2 spike pseudotypes) was noticed (Figure 4A). A similar observation was made using DC-SIGN expressing DC-THP-1 cells

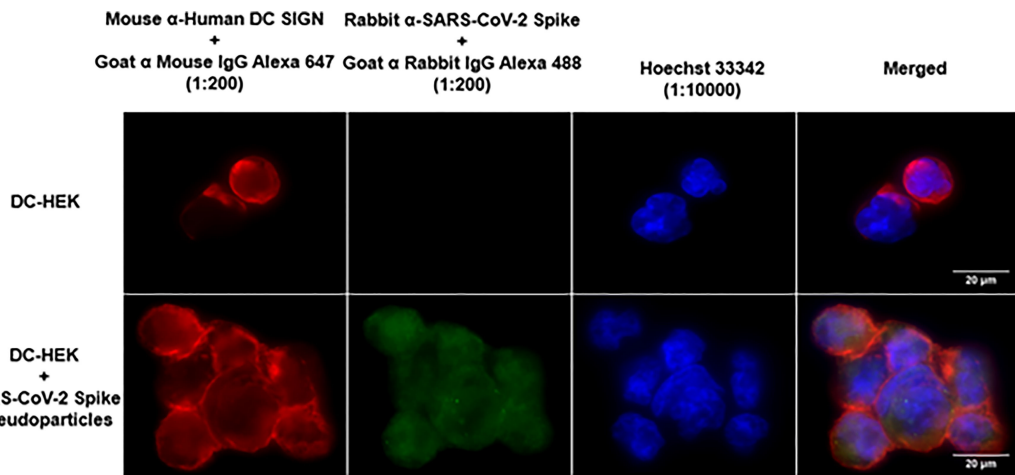


FIGURE 2

Binding of SARS-CoV-2 Spike-Pseudotypes to DC-SIGN expressing cells. DC-HEK cells were incubated with SARS-CoV-2 Spike Pseudotypes for 30 min at 37°C. Spike Pseudotypes challenged DC-HEK cells were fixed with 4% paraformaldehyde, washed, and blocked with 5% FCS. The cells were probed with rabbit anti-SARS-CoV-2 Spike antibody and mouse anti-DC-SIGN to detect the presence of Spike-Pseudotypes and DC-SIGN expressed on the cells, respectively. Alexa Fluor 647 conjugated goat anti-mouse antibody (Abcam), Alexa fluor 488 conjugated goat anti-rabbit antibody (Abcam), and Hoechst (Invitrogen, Life Technologies) were used to detect the primary antibodies and nucleus.

compared to untreated controls. rfhSP-D treatment increased the transduction effectiveness of the pseudotypes in DC-THP-1 cells by ~ 90% (Figure 4B).

### rfhSP-D modulates pro-inflammatory cytokines and chemokines response in SARS-CoV-2 spike protein challenged DC-HEK cells

Pro-inflammatory cytokines and chemokines such as TNF- $\alpha$ , IFN- $\alpha$ , RANTES, and NF- $\kappa$ B transcription factors characterise SARS-CoV-2 infection in the lower respiratory epithelium that express DC-SIGN. DC-HEK cells were challenged with SARS-CoV-2 Spike protein pre-incubated with rfhSP-D to assess the effect of rfhSP-D on the pro-inflammatory cytokines/chemokines released during SARS-CoV-2 infection. The total RNA extracted from the cells was then used in qRT-PCR, with cells challenged with SARS-CoV-2 Spike protein that had not been treated with rfhSP-D serving as the control. rfhSP-D treatment decreased mRNA levels of TNF- $\alpha$ , IFN- $\alpha$ , RANTES, and NF- $\kappa$ B in DC-HEK cells that were challenged with Spike protein. TNF- $\alpha$  mRNA levels were reduced by (~ -3.3 log<sub>10</sub>) (Figure 5C), while IFN- $\alpha$  mRNA levels were downregulated (~ -2.1 log<sub>10</sub>) (Figure 5B). As RANTES is induced by detection of viral components within infected cells, rfhSP-D treatment reduced the mRNA levels of RANTES in DC-HEK cells challenged with Spike (~ -1.3 log<sub>10</sub>) (Figure 5D).

Antiviral cytokines/chemokines are regulated by the transcription factor NF- $\kappa$ B; NF- $\kappa$ B mRNA levels were also reduced (~ -1.2 log<sub>10</sub>) (Figure 5A).

### Modulation of immune response in SARS-CoV-2 spike protein-challenged DC-THP-1 cells by rfhSP-D

Lung macrophages secrete pro-inflammatory mediators such as IL-1, IL-6, IL-8, and TNF- $\alpha$  in response to SARS-CoV-2 infection. To further understand the role of rfhSP-D in modulating the production of pro-inflammatory cytokines/chemokines from lung macrophage expressing DC-SIGN during SARS-CoV-2 infection, rfhSP-D treated/untreated SARS-CoV-2 Spike protein was used to challenge DC-THP-1 cells. qRT-PCR was used to assess the mRNA levels of pro-inflammatory cytokines and chemokines in cells after treatment at 6h and 12h time points (Figure 6). In DC THP-1 cells challenged with Spike protein, rfhSP-D treatment reduced mRNA levels of IL-1, IL-6, IL-8, TNF- $\alpha$ , and NF- $\kappa$ B (Figure 6). mRNA levels of NF- $\kappa$ B at 6h were slightly reduced (~ -1 log<sub>10</sub>). At 12 h, it was significantly downregulated (~ -4 log<sub>10</sub>) in rfhSP-D treated DC-THP-1 cells challenged with Spike protein (Figure 6A). Cells challenged with Spike protein and treated with rfhSP-D at 6h and 12h exhibited a reduction in the gene expression levels of TNF- $\alpha$  (~ -3.1 log<sub>10</sub> and ~ -6.8 log<sub>10</sub>, respectively) (Figure 6B). In rfhSP-D treated DC-THP-1 cells

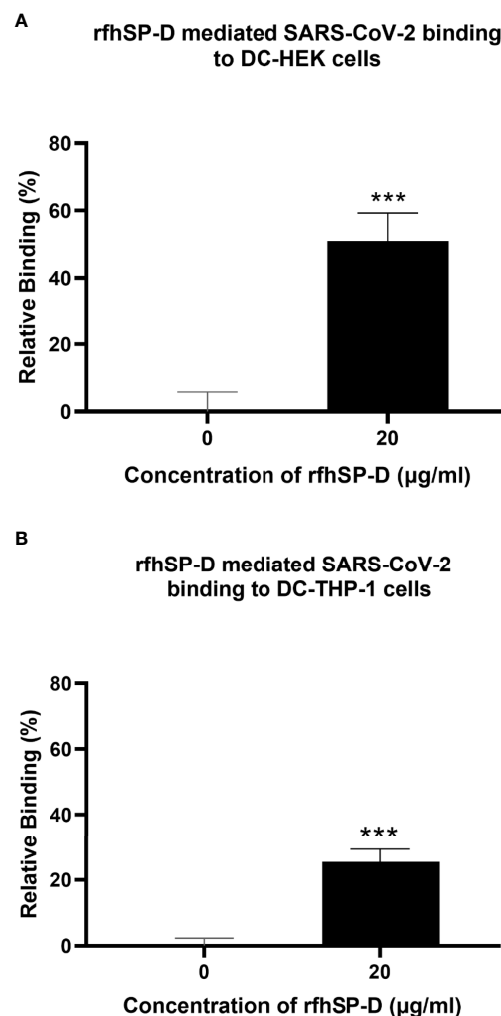


FIGURE 3

rfhSP-D promotes interaction between SARS-CoV-2 Spike Pseudotypes and DC-SIGN expressing cells. DC-HEK cells (A) and DC-THP-1 cells (B) were treated with rfhSP-D and SARS-CoV-2 Spike-Pseudotypes. The cell binding was analysed using Alexa Fluor 488 (FTIC) and Alexa Fluor 647 (APC); the fluorescence intensity was measured using a GloMax 96 Microplate Luminometer (Promega). An increased fluorescence intensity was observed in DC-HEK and DC-THP-1 cells treated with 20 µg/ml of rfhSP-D compared to cells challenged with Spike pseudotypes alone. Experiments were conducted in triplicates, and error bars represent  $\pm$  SEM. Unpaired t-test was used to calculate the significance (\* $p < 0.05$ , \*\* $p < 0.01$ , and \*\*\* $p < 0.001$ ) ( $n = 3$ ). (0, untreated sample; 20, treated sample).

challenged with Spike protein, IL-1 $\beta$  mRNA levels were reduced ( $\sim -2.5 \log_{10}$ ) after 6 h and ( $\sim -4 \log_{10}$ ) 12 h after treatment (Figure 6C). Furthermore, IL-6 levels were significantly downregulated at 12h ( $-5 \log_{10}$ ) in rfhSP-D treated DC-THP-1 cells challenged with Spike protein (Figure 6D). Reduced levels of IL-8 at 6h ( $\sim -2.3 \log_{10}$ ) and 12h ( $\sim -4.8 \log_{10}$ ) were detected in DC-THP-1 cells challenged with Spike protein and treated with rfhSP-D (Figure 6E). MHC class II molecules play a key role in bridging innate and adaptive immunity during anti-viral immune response. rfhSP-D reduced MHC class II expression levels at 6 ( $-2 \log_{10}$ ) and 12h ( $-2.7 \log_{10}$ ) in DC-THP-1 cells challenged with Spike protein (Figure 6F).

## SP-D interacts with RBD and DC-SIGN interacts with NTD of SARS-CoV-2 spike protein

DC-SIGN and SP-D are known to interact through their CRDs (25). This interaction was observed in complex A (docked pose 2) of the current study (Figure 7A; Table 2). The binding site of DC-SIGN (CRD) and Spike protein is not known; therefore, a blind docking approach was attempted to generate complex B. Analysis of the top ranked docked pose of complex B revealed that NTD (N-terminal domain) of spike protein interacted with the CRD domain of DC-SIGN (Figure 7B;

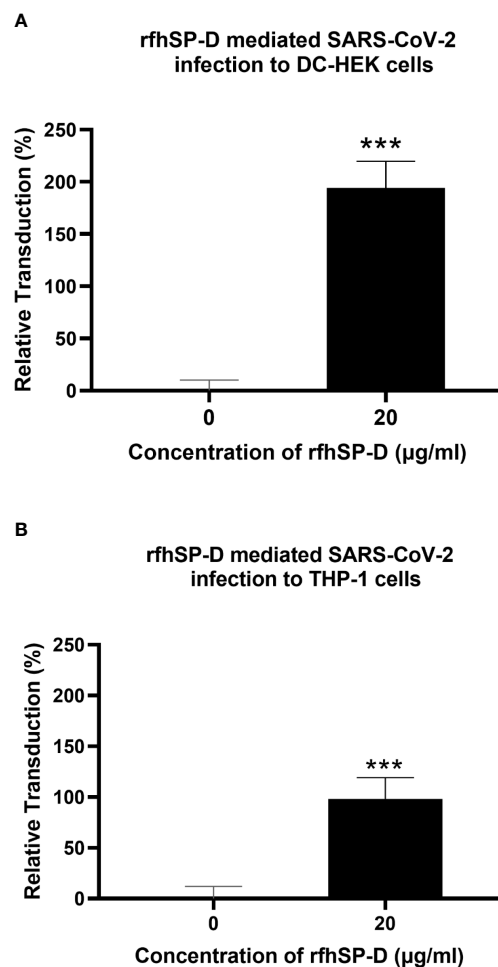


FIGURE 4

rfhSP-D enhances SARS-CoV-2 Spike pseudotype transduction by DC-HEK and DC-THP-1 cells. Purified Spike pseudotypes were used to transduce DC-HEK (A) and DC-THP-1 cells (B), and the luciferase reporter activity was measured. Higher levels of luciferase reporter activities were observed in DC-HEK and DC-THP-1 cells when treated with 20 µg/ml of rfhSP-D compared to cells challenged with Spike pseudotypes only. Experiments were conducted in triplicates, and error bars represent  $\pm$  SEM. Unpaired t-test was used calculate the significance (\* $p < 0.05$ , \*\* $p < 0.01$ , and \*\*\* $p < 0.001$ ) ( $n = 3$ ).

Table 2). Since it was known that Spike protein interacted with SP-D through its receptor binding domain (RBD) (26), we postulated that Spike protein could interact with both SP-D and DC-SIGN (CRD) through two distinct RBD and NTD domains, respectively. This inference is further supported by the *in vitro* observation that binding of DC-SIGN to Spike protein was enhanced by rfhSP-D (Figure 1C). Tripartite complex was generated by docking complex A (DC-SIGN and SP-D) with Spike protein. The top two docked poses (complexes C1 and C2) were analysed for intermolecular interactions (Figure 8; Table 2). In both C1 (Figure 8A) and C2 (Figure 8B) complexes, DC-SIGN (CRD) interacted with NTD domain of Spike protein. In C1, there were no molecular interactions between Spike protein and rfhSP-D (Figure 8A;

Table 2). In C2, Spike protein interacted with rfhSP-D through RBD (Figure 8B; Table 2).

### SP-D stabilises DC-SIGN and SARS-CoV-2 spike protein interaction

MD simulations were performed to assess the effect of SP-D on DC-SIGN (CRD) and Spike protein interaction. The root mean square deviation (RMSD) of complexes C1 and C2 was less than complex B through the course of simulation, indicating that the binding of SP-D enhances the stability of DC-SIGN and spike interaction (Figure 9A). This observation was supported by potential energy (PE), distance, and H-bond profile. Trajectory

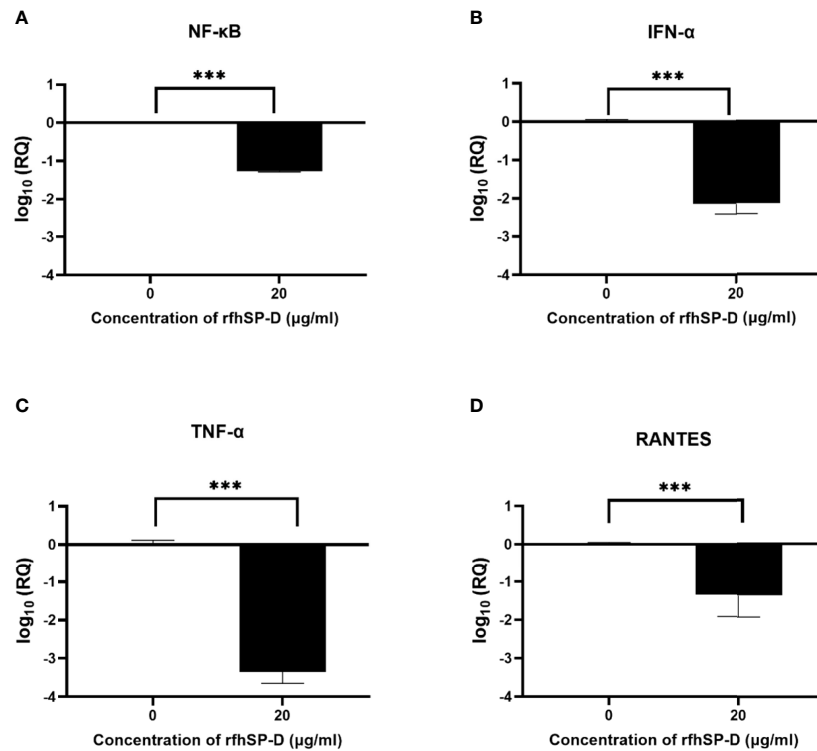


FIGURE 5

rfhSP-D downregulates pro-inflammatory cytokines and chemokines in DC-HEK cells. SARS-CoV-2 Spike protein incubated with 20µg/ml of rfhSP-D was used to challenge DC-HEK cells. Cells were harvested at 6 h to analyse the expression of cytokines. RNA was purified and converted into cDNA. The gene expression levels of NF-κB (A), IFN-α (B), TNF-α (C), and RANTES (D) were assessed using RT-qPCR. 18S rRNA was used as an endogenous control. The relative expression (RQ) was calculated using cells challenged with Spike protein untreated with rfhSP-D as the calibrator. The RQ value was calculated using  $RQ = 2^{-\Delta\Delta Ct}$ . Assays were conducted in triplicates, and error bars represent  $\pm$  SEM. Significance was determined using the two-way ANOVA test (\*\*p < 0.01, and \*\*\*p < 0.0001) (n = 3).

analysis of PE, intermolecular distance and H-bonds between DC-SIGN and spike indicated higher stability of C1 and C2 complexes as compared to B (Figures 9B, 10A–C, 10D–F). Between the tripartite complexes, C1 exhibited slightly better stability than C2 (Figures 9, 10). These analyses suggest that the interaction of DC-SIGN and spike gets stabilized in the presence of SP-D.

## Discussion

Specific molecular structures on the surfaces of pathogens (PAMP) are directly recognised by pattern recognition receptors (PRRs) (4). PRRs serve as a link between nonspecific and specific immunity. PRRs can exert nonspecific anti-infection, anti-tumour, and other immune-protective actions by recognising and binding non-self ligands (52). CLRs are PRRs, which use calcium to recognise carbohydrate residues on harmful bacteria and viruses (53). DC-SIGN and SP-D are CLRs that play an important role in anti-viral immunity, including SARS-CoV-2,

the causative agent of coronavirus induced illness 2019 (COVID-19) (54, 55). The availability of virus receptors and entry cofactors on the surface of host cells determines tissue tropism for many viruses (56, 57). We found rfhSP-D potentiated SARS-CoV-2 binding and entry to DC-SIGN expressing cells. Furthermore, rfhSP-D treatment was also found to impair downstream signalling induced by the binding of Spike protein to DC-SIGN resulting in the downregulation of pro-inflammatory mediators' gene expression. However, further experiments using DC-SIGN expressing cells challenged with rfhSP-D treated SARS-CoV-2 clinical isolates need to be undertaken to confirm the rfhSP-D mediated cytokine modulation observed. Our findings elucidate a novel interaction between rfhSP-D, DC-SIGN and SARS-CoV-2, which may uncover therapeutic potential for controlling SARS-CoV-2 infection and subsequent cytokine storm.

DC-SIGN, widely expressed on DCs and alveolar macrophages in the lungs, interacts with SARS-CoV-2 through Spike protein (47). DC-SIGN has previously been shown to interact with SARS-CoV, HIV-1 and Ebola virus (41, 58, 59).

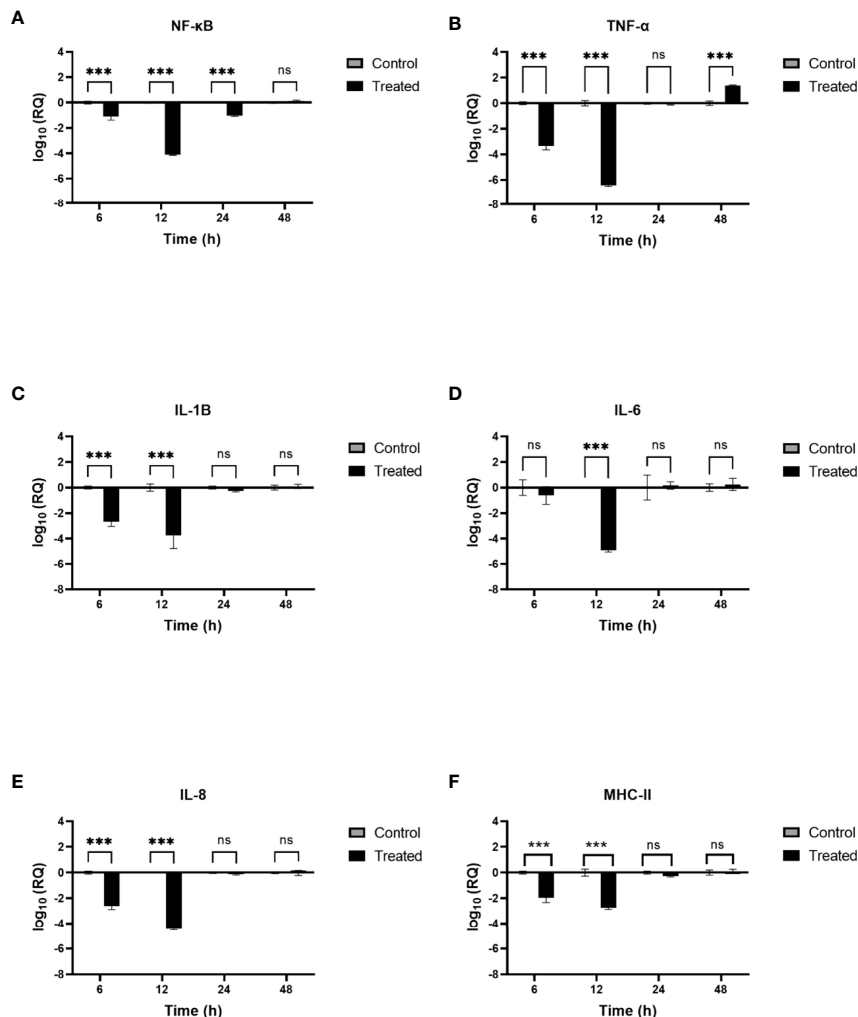


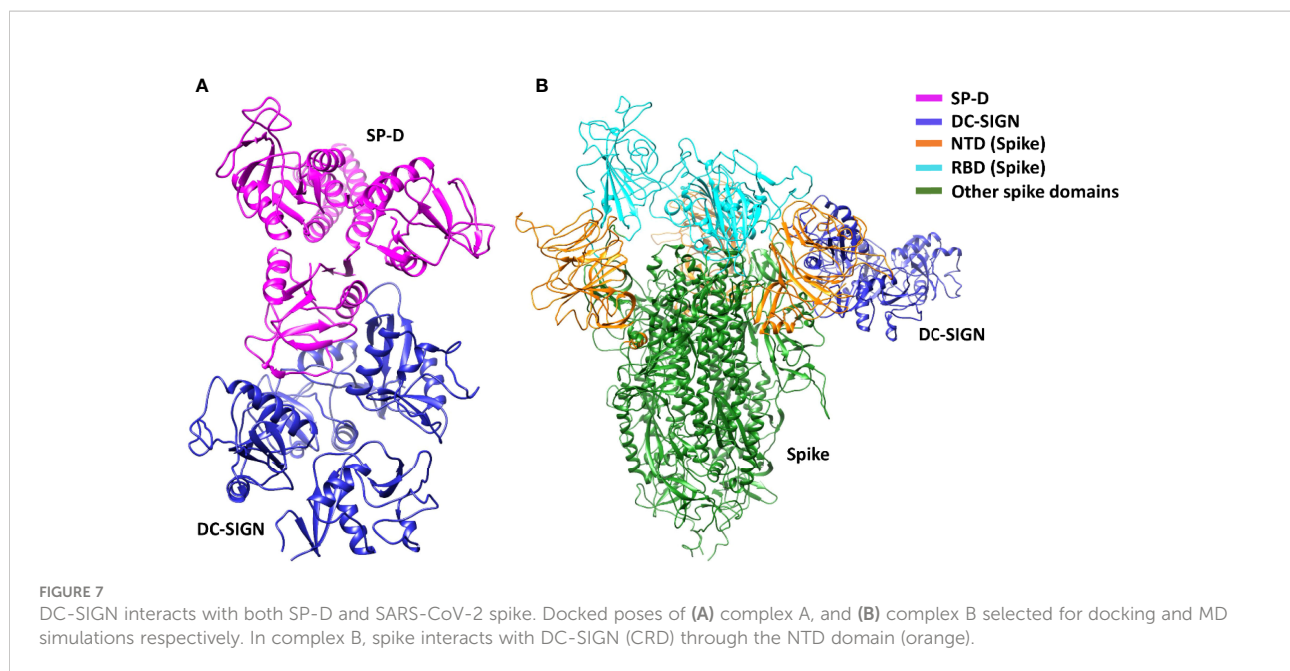
FIGURE 6

rfhSP-D modulates immune response in DC-THP-1 cells. SARS-CoV-2 Spike protein incubated with 20 $\mu$ g/ml of rfhSP-D was used to challenge DC-THP-1 cells. Cells were harvested at 6h, 12h, 24h, and 48h to analyse the expression of cytokines and MHC class II. Cells were lysed, and purified RNA was converted into cDNA. The expression levels of NF- $\kappa$ B (A), TNF- $\alpha$  (B), IL-1 $\beta$  (C), IL-6 (D), IL-8 (E) and MHC class II (F) were measured using RT-qPCR, and the data were normalised against 18S rRNA expression as a control. Experiments were conducted in triplicates, and error bars represent  $\pm$  SEM. The relative expression (RQ) was calculated using cells challenged with Spike protein untreated with rfhSP-D as the calibrator.  $\text{RQ} = 2^{-\Delta\Delta\text{Ct}}$  was used to calculate the RQ value. Significance was determined using the two-way ANOVA test (\*\* $p < 0.01$ , and \*\*\*\* $p < 0.0001$ ) ( $n = 3$ ).

SARS-CoV uses DC-SIGN for entry into DCs (47). In addition to its role as a virus attachment receptor, DC-SIGN has been implicated in triggering DC maturation, myeloid cell cytokine response, and T cell priming. Another CLR, SP-D, has been shown to have antiviral properties against SARS-CoV-2, HIV-1 and IAV infection (43, 45). We previously demonstrated that rfhSP-D reduced SARS-CoV-2 S1 protein binding to HEK293T cells overexpressing ACE2 receptors and infection in A549 cells by restricting viral entry (27). However, the role of SP-D in SARS-CoV-2 and DC-SIGN interaction is not well understood.

The binding of the SARS-CoV-2 Spike protein to the host cell *via* the ACE2 receptor is one of the critical steps in the SARS-

CoV-2 infection (60). The receptor binding motif (RBM) (455-508) within the RBD of S1 protein interacts with the virus-binding residues consisting of Lys31, Glu35, and Lys353 of dimeric ACE2 (61). Although the sequence of events around the Spike protein/ACE2 association is becoming more evident, additional factors that aid infection remains unknown, for example, SARS-CoV-2 transport to the ACE2 receptor (36). Both SARS-CoV and SARS-CoV-2 Spike proteins have the same affinity for ACE2, but the transmission rate are drastically different (37). It has been suggested that the higher transmission rate of SARS-CoV-2 compared to SARS-CoV is due to more efficient viral adherence *via* host-cell attachment



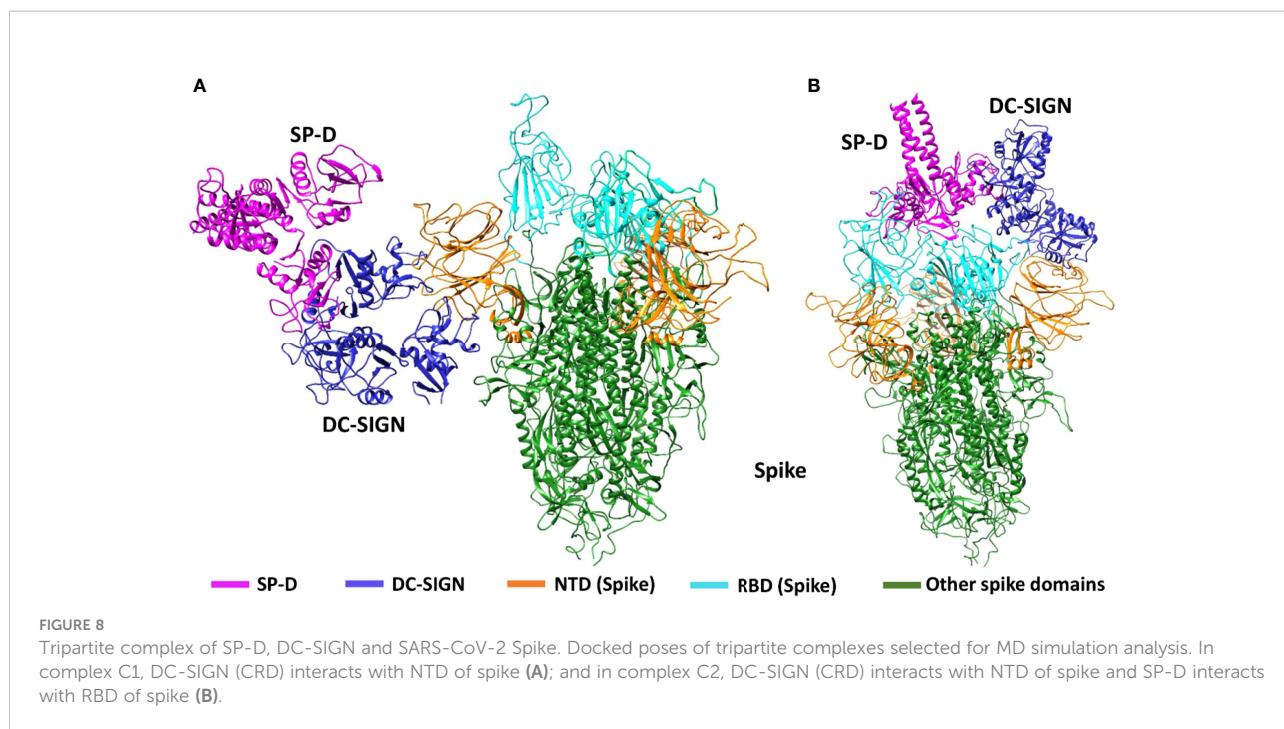
factors, leading to improved infection of ACE2 expressing cells (38, 39). DC-SIGN has also been identified as a SARS-CoV Spike protein receptor capable of enhancing cell entry in ACE2<sup>+</sup> pneumocytes *via* DC transfer (40). Recently, it has been shown that DC-SIGN binds to SARS-CoV-2 Spike protein and promotes trans-infection (20). In this study, we investigated the potential of rfhSP-D in inhibiting SARS-CoV-2 binding and entry into DC-SIGN expressing cells. Targeting viral entry into a host cell is a new approach for developing antiviral drugs that could interfere with viral propagation early in the SARS-CoV-2 viral cycle (62). We have independently confirmed the previously reported interaction between SARS-CoV-2 and rfhSP-D or DC-SIGN (20, 26, 27).

Here, we show that rfhSP-D enhances the binding of the SARS-CoV-2 Spike to DC-SIGN. This is further confirmed by

*in-silico* molecular dynamics studies which indicate that SP-D stabilises the binding interactions between DC-SIGN CRD and N-terminal domain of SARS-CoV-2 Spike protein. The consequence of this tripartite complex involving DC-SIGN, SARS-CoV-2 Spike protein and rfhSP-D on viral infection was assessed using SARS-CoV-2 Spike protein-expressing replication-incompetent lentiviral pseudotyped viral particles since they are a safe alternative to the live virus. Using these pseudotypes, we demonstrate that rfhSP-D enhances spike protein binding and uptake in DC-SIGN expressing cells. A significant increase in spike protein binding and transduction was observed compared to untreated samples (Cells + SARS-CoV-2) to rfhSP-D (20 µg/ml) treatment. It has been shown previously that SP-D enhances the clearance of IAV from the lung *in vivo* (44). Similarly, the interaction of rfhSP-D with DC-

TABLE 2 Interaction analysis of the docked complexes of DC-SIGN, spike and SP-D.

Complex	DockedPose	Receptor	Ligand	H-bonding residues	
				Receptor	Ligand
A	2	DC-SIGN	SP-D	PHE262, GLN264, GLN274, ARG275, ASN362, SER383 CYS384	GLN263, GLN281, GLN282, ASN288, ASN316, TRP317, GLY320, ASP325
B	1	DC-SIGN	Spike	CYS253, HIS254, LYS285, GLY288, LEU321, ASN322, GLN323, GLU324, GLU353, ASN370, LYS379, SER380, ALA382, SER383	TYR28, ASN30, PHE58, PHE59, ASN61, VAL83, ASN87, ARG237, GLN239, PRO527, LYS529, SER530, THR531, ASN532, LEU533
C1 (A + Spike)	1	DC-SIGN	Spike	LEU321, GLY325, THR326, ARG345, ASN349, ASN350	ALA27, TYR28, HIS69, SER98, ASN211, ARG214
C2 (A + Spike)	2	DC-SIGN	Spike	ASN276, ASN322, GLN328, VAL330, GLY352, ASP355, ASN370	ASP111, GLU132, ASP138, PHE140, TYR160, ALA163, TYR248, THR250, SER254
			Spike	SP-D	ARG408, GLN409, VAL445, GLY502

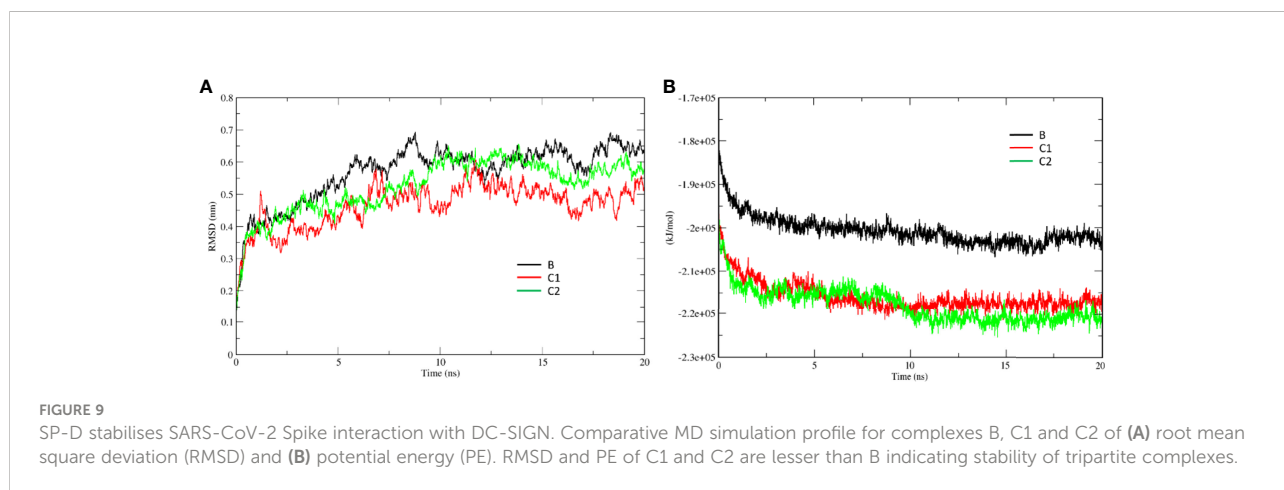


SIGN may augment SARS-CoV-2 binding and uptake by macrophages, indicating that rhfSP-D may promote the clearance of SARS-CoV-2 *via* DC-SIGN.

The effect of rhfSP-D on gene expression levels of pro-inflammatory mediators in SARS-CoV-2 Spike protein challenged DC-HEK and DC-THP-1 cells were investigated in the current study. To our knowledge, this is the first study looking at the impact of rhfSP-D on DC-SIGN cells challenged with SARS-CoV-2. rhfSP-D showed anti-inflammatory effects on DC-SIGN expressing cells, as evident from the reduction in the levels of cytokines/chemokines such as TNF- $\alpha$  and IL-8.

DC-SIGN present on DC surface has been implicated in activating the STAT3 pathway during viral infection (63, 64).

STAT3 plays a crucial role in activating transcription factor NF- $\kappa$ B in SARS-CoV-2 infection in myeloid cells, which may trigger subsequent cytokine production and stimulate pathological inflammation (65, 66). The activation of NF- $\kappa$ B in viral infection induces gene expression of a wide range of cytokines (e.g., IL-1, IL-2, IL-6, IL-12, TNF- $\alpha$ , LT- $\alpha$ , LT- $\beta$ , and GM-CSF), and chemokines (e.g., IL-8, MIP-1, MCP1, RANTES, and eotaxin) (67). These inflammatory mediators are involved in antiviral immunity and essential for infection resistance (67). Nevertheless, in moderate and severe SARS-CoV 2 infection, the activation of NF- $\kappa$ B in various cells, including macrophages in the lungs, liver, kidney, central nervous system, gastrointestinal system, and cardiovascular system, results in the production of



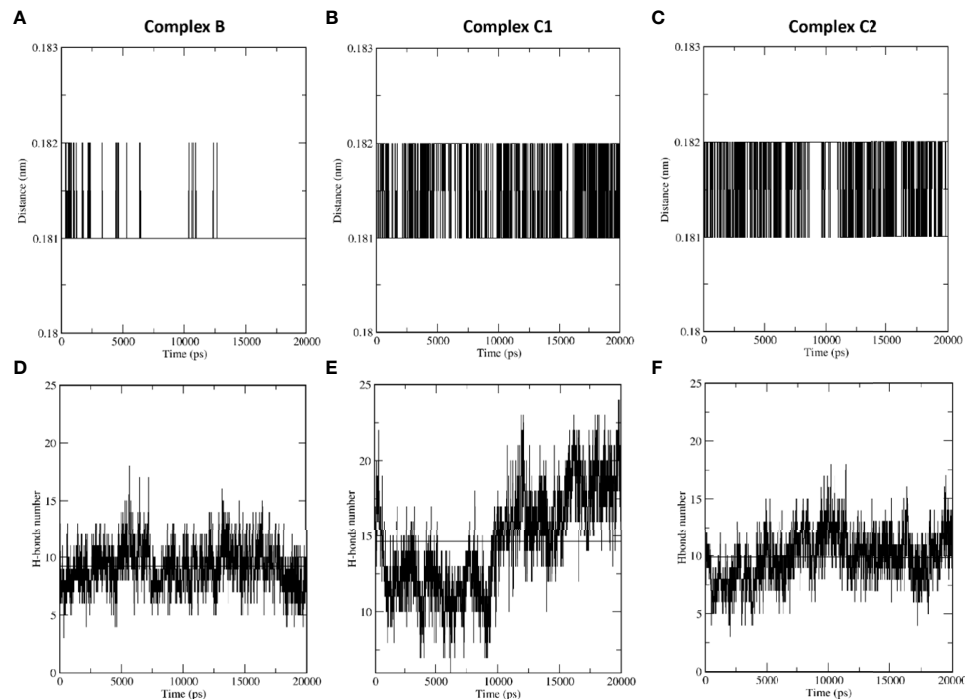


FIGURE 10

SP-D stabilises SARS-CoV-2 Spike interaction with DC-SIGN. Comparative MD simulation profile of complexes B, C1 and C2 for average distance (A–C) and H-bonds (D–F) between DC-SIGN and spike. The intermolecular distance is conserved across the simulation period for tripartite complexes C1 and C2 as compared to complex (B). The number of intermolecular H-bonds between DC-SIGN and spike are also higher for complexes C1 and C2 as compared to (B). These observations indicate the stabilising effect of SP-D on spike and DC-SIGN (CRD) interaction.

IL-1 $\beta$ , IL-6, IL-8, and TNF- $\alpha$  (68). This may result in cytokine storm and organ failure, and consequently, morbidity and mortality (68, 69). Immunomodulation at the level of NF- $\kappa$ B activation and inhibitors of NF- $\kappa$ B degradation may reduce the cytokine storm and lessen the severity of SARS-CoV-2 infection (68, 70). Pro-inflammatory mediators have been shown to be induced by SARS-CoV-2 Spike protein in THP-1 cells as *in vitro* model for lung macrophages (71). In this study, the inflammatory response was evaluated *via* measuring the gene expression levels of NF- $\kappa$ B in DC-HEK and DC-THP-1 challenged with SARS-CoV-2 spike protein. Our findings show that rfhSP-D downregulates the gene expression levels of NF- $\kappa$ B in DC-HEK and DC-THP-1 challenged with SARS-CoV-2 Spike protein. Thus, rfhSP-D suppresses pro-inflammatory immune response in DC-SIGN expressing immune cells.

Another critical element in the pathophysiology of SARS-CoV-2 infection is TNF- $\alpha$ , which is produced in the airway by macrophages, mast cells, T cells, epithelial cells, and smooth muscle cells (4, 72). TNF- $\alpha$  synthesis is predominantly stimulated by PAMPs through NF- $\kappa$ B activation (73). Various studies have reported that patients with severe SARS-CoV-2 infection display elevated plasma levels of TNF- $\alpha$  (74–76). This causes airway inflammation due to recruitment of mostly

neutrophils (77). In addition, TNF- $\alpha$  stimulates the production of cytokines like IL-1 $\beta$  and IL-6 (78). DC-HEK and DC-THP-1, challenged with SARS-CoV-2 Spike protein, pre-treated with rfhSP-D, caused downregulation in the gene expression levels of TNF- $\alpha$  as compared to rfhSP-D-untreated cells. The results suggest an important immunomodulatory role of rfhSP-D in SARS-CoV-2-mediated inflammation.

IL-1 $\beta$  is released following activation of the inflammasome in response to a variety of infections, including SARS-CoV-2 (79). When compared to non-infected subjects, high levels of IL-1 $\beta$  were found in the plasma of severe as well as moderate CoVID-19 cases (75). Cell pyroptosis is a highly inflammatory form of programmed cell death typically seen with cytopathic viruses. An increase in IL-1 $\beta$  production is a downstream sign of pyroptosis (80). As a result, pyroptosis plays an essential role in the pathogenesis of SARS-CoV-2 and is a likely trigger for the uncontrolled inflammatory response (81). In this study, DC-THP-1 cells challenged by Spike protein, pre-treated with rfhSP-D, exhibited low mRNA levels of IL-1 $\beta$  as compared to the control. Thus, rfhSP-D may reduce the unnecessary inflammatory response to SARS-CoV-2 infection *via* reduction in IL-1 $\beta$  production.

IL-6 is a glycoprotein that regulates the immune system, haematopoiesis, inflammation and is a major player in SARS-

CoV-2 infection (82). Many cell types, including T and B lymphocytes, monocytes/macrophages, DCs fibroblasts and endothelial, express IL-6 (82, 83). A higher level of IL-6 in the plasma has been linked with the severity of SARS-CoV-2 infection (84, 85). rfhSP-D-treated DC-THP-1 cells challenged by Spike protein showed downregulation of IL-6 transcripts as compared with untreated cells. This suggests a role for SP-D in preventing IL-6 immunopathogenesis due to SARS-CoV-2.

IFN- $\alpha$  is a cytokine mainly secreted by virus-infected cells associated with stimulation of immune response and limiting viral infection (86). Nonetheless, elevated expression levels of IFN-stimulated genes (ISGs) are triggered by SARS-CoV 2, which exhibits immunopathogenic potential (58). IFN- $\alpha$  expression levels are downregulated in rfhSP-D treated DC-HEK cells challenged with SARS-CoV-2 spike protein compared to the control. The results suggest rfhSP-D may elevate immunopathological potential of SARS-CoV-2.

Another element that may aid viral infectivity of DCs is MHC class II molecule. SARS-CoV-2 has been shown to upregulate MHC class II gene expression (87). High expression level of MHC class II molecules on the surface of antigen-presenting cells is crucial for regulating and inducing an adaptive immune response to respiratory viruses (88). However, limited-expression levels of MHC class II molecules on type II alveolar cells and macrophages improve respiratory viral disease outcomes (89). The binding of SARS-CoV-2 Spike protein to THP-1 cells polarises towards M1-like phenotype together with an increase in MHC class II molecules (71). DC-THP-1 cells challenged with SARS-CoV-2 Spike protein and treated with rfhSP-D showed downregulation of MHC class II mRNA expression levels. Thus, SP-D may have a role in modulating antigen presentation in order to avoid an unwanted and exaggerated adaptive immune response.

Chemokines, such as IL-8 and RANTES, are vital for recruiting inflammatory cells from the intravascular space across the endothelium and epithelium to the inflammation site (90). IL-8, commonly known as CXCL8, is a crucial mediator of inflammation with a direct chemotactic and priming action on neutrophils (91). In addition, IL-8 induces NETosis (Neutrophil extracellular traps/NETs). SARS-CoV-2 infected patients exhibit elevated levels of citrullinated histone H3 (Cit-H3) and myeloperoxidase (MPO)-DNA, which are specific markers of NETs that may cause organ damage (92). DC-THP-1 challenged with Spike protein and treated with rfhSP-D had low mRNA levels of IL-8 as compared to the control. There appears a role for SP-D in preventing IL-8-associated pathogenesis due to SARS-CoV-2.

RANTES is a chemokine that has been linked with enhanced pathogenicity and mortality in SARS-CoV-2 infection (93). Compared to healthy control, SARS-CoV-2 infected patients contain higher serum RANTES and IL-6 levels which correlated with severity of CoVID-19 (94). In this study, the mRNA expression levels of RANTES were found to be considerably

downregulated in DC-HEK cells challenged with Spike protein and treated with rfhSP-D. Thus, SP-D may modulate leukocyte recruitment to infection areas.

Thus, the results of this study help support the hypothesis that rfhSP-D facilitates the binding and uptake of SARS-CoV-2 pseudotypes and downregulates the virus-induced inflammatory response in DC-SIGN expressing cells. However, further study is required to assess the expression of DC-SIGN in individuals with mild/severe SARS-CoV-2 infection. SARS-CoV-2 is also known to affect organs other than the lungs. Thus, it is imperative to study the possibility of viral transfer to secondary sites *via* DC-SIGN and the effect of SP-D on this process. Furthermore, the interaction of rfhSP-D and/or DC-SIGN with the Spike protein of various SARS-CoV-2 variants and lineages need to be investigated to explore the viability of rfhSP-D as a universal treatment against SARS-CoV-2 infection. Additionally, the effects of rfhSP-D mediated DC-SIGN: SARS-CoV-2 interaction needs to be studied in the lung microenvironment using established animal models for COVID-19 such as Hamsters, Mouse, Ferret, Mink, Tree Shrew, and Non-human Primates.

In conclusion, our study reveals that rfhSP-D can effectively increase the binding and uptake of SARS-CoV-2 by DC-SIGN expressing cells. We also show that rfhSP-D causes substantial downregulation of pro-inflammatory cytokines such as IL-1 $\beta$ , TNF- $\alpha$  and IL-6, and chemokines like IL-8 and RANTES, in DC-SIGN expressing cells. These findings provide further credence to the evidence that rfhSP-D has a significant protective role against lung viral infection and immunopathogenesis. Our data suggests that rfhSP-D stabilises the interaction between SARS-CoV-2 Spike protein and DC-SIGN and helps in enhancing viral uptake by macrophages, suggesting an additional role for rfhSP-D in SARS-CoV-2 infection.

## Data availability statement

The datasets presented in this study can be found in online repositories. The names of the repository/repositories and accession number(s) can be found below: <https://biorxiv.org/cgi/content/short/2022.05.16.491949v1>.

## Author contributions

NB, PV, CK, MM, VM, and NT carried out crucial experiments; PV, TM, SI-T, and UK supervised most experiments; MS, RB, DM, MM, and NT generated crucial reagents; PV and UK produced the draft. All authors contributed to the article and approved the submitted version.

## Funding

CK and SI-T are grateful to the grants received from the Department of Biotechnology, India [No. BT/PR40165/BTIS/

137/12/2021]. NT and MM are funded by the Wellcome Trust (GB-CHC-210183).

## Conflict of interest

The authors declare that the research was conducted in the absence of any commercial or financial relationships that could be construed as a potential conflict of interest.

## References

1. Takeuchi O, Akira S. Pattern recognition receptors and inflammation. *Cell* (2010) 140(6):805–20. doi: 10.1016/j.cell.2010.01.022
2. Akira S, Uematsu S, Takeuchi O. Pathogen recognition and innate immunity. *Cell* (2006) 124(4):783–801. doi: 10.1016/j.cell.2006.02.015
3. Kumar H, Kawai T, Akira S. Pathogen recognition in the innate immune response. *Biochem J* (2009) 420(1):1–16. doi: 10.1042/BJ20090272
4. Akira S. Pathogen recognition by innate immunity and its signaling. *Proc Japan Academy Ser B* (2009) 85(4):143–56. doi: 10.2183/pjab.85.143
5. Stambach NS, Taylor ME. Characterization of carbohydrate recognition by langerin, a c-type lectin of langerhans cells. *Glycobiology* (2003) 13(5):401–10. doi: 10.1093/glycob/cwg045
6. Drickamer K, Taylor ME. Recent insights into structures and functions of c-type lectins in the immune system. *Curr Opin Struct Biol* (2015) 34:26–34. doi: 10.1016/j.sbi.2015.06.003
7. Qian C, Cao X. Dendritic cells in the regulation of immunity and inflammation. *Semin Immunol* (2018) 35:3–11. doi: 10.1016/j.smim.2017.12.002
8. Worbs T, Hammerschmidt SI, Förster R. Dendritic cell migration in health and disease. *Nat Rev Immunol* (2017) 17(1):30–48. doi: 10.1038/nri.2016.116
9. Geijtenbeek TB, Torensma R, van Vliet SJ, van Duijnhoven GC, Adema GJ, van Kooyk Y, et al. Identification of DC-SIGN, a novel dendritic cell-specific ICAM-3 receptor that supports primary immune responses. *Cell* (2000) 100(5):575–85. doi: 10.1016/S0092-8674(00)80693-5
10. Pednekar L, Pandit H, Paudyal B, Kaur A, Al-Mozaini MA, Kouser L, et al. Complement protein C1q interacts with DC-SIGN via its globular domain and thus may interfere with HIV-1 transmission. *Front Immunol* (2016) 7:600. doi: 10.3389/fimmu.2016.00600
11. Mitchell DA, Fadden AJ, Drickamer K. A novel mechanism of carbohydrate recognition by the c-type lectins DC-SIGN and DC-SIGNR: Subunit organization and binding to multivalent ligands. *J Biol Chem* (2001) 276(31):28939–45. doi: 10.1074/jbc.M104565200
12. Hodges A, Sharrocks K, Edelman M, Baban D, Moris A, Schwartz O, et al. Activation of the lectin DC-SIGN induces an immature dendritic cell phenotype triggering rho-GTPase activity required for HIV-1 replication. *Nat Immunol* (2007) 8(6):569–77. doi: 10.1038/ni1470
13. Frison N, Taylor ME, Soilleux E, Bousser M-T, Mayer R, Monsigny M, et al. Oligosaccharide-based oligosaccharide clusters: Selective recognition and endocytosis by the mannose receptor and dendritic cell-specific intercellular adhesion molecule 3 (ICAM-3)-Grabbing nonintegrin. *J Biol Chem* (2003) 278(26):23922–9. doi: 10.1074/jbc.M302483200
14. Halary F, Amara A, Lortat-Jacob H, Messerle M, Delaunay T, Houles C, et al. Human cytomegalovirus binding to DC-SIGN is required for dendritic cell infection and target cell trans-infection. *Immunity* (2002) 17(5):653–64. doi: 10.1016/S1074-7613(02)00447-8
15. Alvarez CP, Lasala F, Carrillo J, Muñoz O, Corbí AL, Delgado R. C-type lectins DC-SIGN and I-SIGN mediate cellular entry by Ebola virus in cis and in trans. *J Virol* (2002) 76(13):6841–4. doi: 10.1128/JVI.76.13.6841-6844.2002
16. Carbaugh DL, Baric RS, Lazear HM. Envelope protein glycosylation mediates zika virus pathogenesis. *J Virol* (2019) 93(12):e00113–19. doi: 10.1128/JVI.00113-19
17. Geijtenbeek TB, Kwon DS, Torensma R, Van Vliet SJ, Van Duijnhoven GC, Middel J, et al. DC-SIGN, a dendritic cell-specific HIV-1-binding protein that enhances trans-infection of T cells. *Cell* (2000) 100(5):587–97. doi: 10.1016/S0092-8674(00)80694-7
18. Navarro-Sanchez E, Altmeyer R, Amara A, Schwartz O, Fieschi F, Virelizier JL, et al. Dendritic-Cell-Specific ICAM3-grabbing non-integrin is essential for the productive infection of human dendritic cells by mosquito-Cell-Derived dengue viruses. *EMBO Rep* (2003) 4(7):723–8. doi: 10.1038/sj.embor.embor866
19. Manches O, Frelta D, Bhardwaj N. Dendritic cells in progression and pathology of HIV infection. *Trends Immunol* (2014) 35(3):114–22. doi: 10.1016/j.it.2013.10.003
20. Thépaut M, Luczkowiak J, Vivès C, Labiod N, Bally I, Lasala F, et al. DC/L-SIGN recognition of spike glycoprotein promotes SARS-CoV-2 trans-infection and can be inhibited by a glycomimetic antagonist. *PLoS Pathog* (2021) 17(5):e1009576. doi: 10.1371/journal.ppat.1009576
21. Arroyo R, Grant SN, Colombo M, Salvioni L, Corsi F, Truffi M, et al. Full-length recombinant hSP-d binds and inhibits SARS-CoV-2. *Biomolecules* (2021) 11(8):1114. doi: 10.3390/biom11081114
22. Singh M, Madan T, Waters P, Parida SK, Sarma PU, Kishore U. Protective effects of a recombinant fragment of human surfactant protein d in a murine model of pulmonary hypersensitivity induced by dust mite allergens. *Immunol Lett* (2003) 86(3):299–307. doi: 10.1016/S0165-2478(03)00033-6
23. Liu M-Y, Zheng B, Zhang Y, Li J-P. Role and mechanism of angiotensin-converting enzyme 2 in acute lung injury in coronavirus disease 2019. *Chronic Dis Trans Med* (2020) 6(2):98–105. doi: 10.1016/j.cdtm.2020.05.003
24. Luan B, Huynh T, Cheng X, Lan G, Wang H-R. Targeting proteases for treating COVID-19. *J Proteome Res* (2020) 19(11):4316–26. doi: 10.1021/acs.jproteome.0c00430
25. Dodagatta-Marri E, Mitchell DA, Pandit H, Sonawani A, Murugaiah V, Idicula-Thomas S, et al. Protein-protein interaction between surfactant protein d and DC-SIGN via c-type lectin domain can suppress HIV-1 transfer. *Front Immunol* (2017) 8:834. doi: 10.3389/fimmu.2017.00834
26. Madan T, Biswas B, Varghese PM, Subedi R, Pandit H, Idicula-Thomas S, et al. A recombinant fragment of human surfactant protein d binds spike protein and inhibits infectivity and replication of SARS-CoV-2 in clinical samples. *Am J Respir Cell Mol Biol* (2021) 65(1):41–53. doi: 10.1165/rcmb.2021-0005OC
27. Hsieh M-H, Beirag N, Murugaiah V, Chou Y-C, Kuo W-S, Kao H-F, et al. Human surfactant protein d binds spike protein and acts as an entry inhibitor of SARS-CoV-2 pseudotyped viral particles. *Front Immunol* (2021) 12:1613. doi: 10.3389/fimmu.2021.641360
28. Dessie ZG, Zewotir T. Mortality-related risk factors of COVID-19: A systematic review and meta-analysis of 42 studies and 423,117 patients. *BMC Infect Dis* (2021) 21(1):1–28. doi: 10.1186/s12879-021-06536-3
29. Abate SM, Checkol YA, Mantefardo B. Global prevalence and determinants of mortality among patients with COVID-19: A systematic review and meta-analysis. *Ann Med Surg* (2021) 64:102204. doi: 10.1016/j.amsu.2021.102204
30. Chen N, Zhou M, Dong X, Qu J, Gong F, Han Y, et al. Epidemiological and clinical characteristics of 99 cases of 2019 novel coronavirus pneumonia in wuhan, China: A descriptive study. *Lancet* (2020) 395(10223):507–13. doi: 10.1016/S0140-6736(20)30211-7
31. Hirabara SM, Serdan TD, Gorjao R, Masi LN, Pithon-Curi TC, Covas DT, et al. SARS-CoV-2 variants: Differences and potential of immune evasion. *Front Cell Infect Microbiol* (2022) p:1401. doi: 10.3389/fcimb.2021.781429
32. Wu Z, McGoogan JM. Characteristics of and important lessons from the coronavirus disease 2019 (COVID-19) outbreak in China: Summary of a report of 72 314 cases from the Chinese center for disease control and prevention. *JAMA* (2020) 323(13):1239–42. doi: 10.1001/jama.2020.2648
33. Ludwig S, Zarbock A. Coronaviruses and SARS-CoV-2: A brief overview. *Anesth Analgesia* (2020) 131(1):93–6. doi: 10.1213/ANE.00000000000004845
34. Shirbhate E, Pandey J, Patel VK, Kamal M, Jawaid T, Gorain B, et al. Understanding the role of ACE-2 receptor in pathogenesis of COVID-19 disease: A potential approach for therapeutic intervention. *Pharmacol Rep* (2021) 73(6):1539–50. doi: 10.1007/s43440-021-00303-6
35. Ni W, Yang X, Yang D, Bao J, Li R, Xiao Y, et al. Role of angiotensin-converting enzyme 2 (ACE2) in COVID-19. *Crit Care* (2020) 24(1):1–10. doi: 10.1186/s13054-020-03120-0

## Publisher's note

All claims expressed in this article are solely those of the authors and do not necessarily represent those of their affiliated organizations, or those of the publisher, the editors and the reviewers. Any product that may be evaluated in this article, or claim that may be made by its manufacturer, is not guaranteed or endorsed by the publisher.

36. Walls AC, Park Y-J, Tortorici MA, Wall A, McGuire AT, Veesler D. Structure, function, and antigenicity of the SARS-CoV-2 spike glycoprotein. *Cell* (2020) 181(2):281–92.e6. doi: 10.1016/j.cell.2020.02.058
37. Petersen E, Koopmans M, Go U, Hamer DH, Petrosillo N, Castelli F, et al. Comparing SARS-CoV-2 with SARS-CoV and influenza pandemics. *Lancet Infect Dis* (2020) 20(9):e238–44. doi: 10.1016/S1473-3099(20)30484-9
38. Sungnak W, Huang N, Bécavin C, Berg M, Queen R, Litvinukova M, et al. SARS-CoV-2 entry factors are highly expressed in nasal epithelial cells together with innate immune genes. *Nat Med* (2020) 26(5):681–7. doi: 10.1038/s41591-020-0868-6
39. Backovic M, Rey FA. Virus entry: Old viruses, new receptors. *Curr Opin Virol* (2012) 2(1):4–13. doi: 10.1016/j.coviro.2011.12.005
40. Yang Z-Y, Huang Y, Ganesh L, Leung K, Kong W-P, Schwartz O, et al. pH-dependent entry of severe acute respiratory syndrome coronavirus is mediated by the spike glycoprotein and enhanced by dendritic cell transfer through DC-SIGN. *J Virol* (2004) 78(11):5642–50. doi: 10.1128/JVI.78.11.5642-5650.2004
41. Marzi A, Gramberg T, Simmons G, Möller P, Rennekamp AJ, Krumbiegel M, et al. DC-SIGN and DC-SIGNR interact with the glycoprotein of marburg virus and the s protein of severe acute respiratory syndrome coronavirus. *J Virol* (2004) 78(21):12090–5. doi: 10.1128/JVI.78.21.12090-12095.2004
42. Mangalmurti N, Hunter CA. Cytokine storms: Understanding COVID-19. *Immunity* (2020) 53(1):19–25. doi: 10.1016/j.immuni.2020.06.017
43. Al-Ahdal MN, Murugiah V, Varghese PM, Abozaid SM, Saba I, Al-Qatani AA, et al. Entry inhibition and modulation of pro-inflammatory immune response against influenza a virus by a recombinant truncated surfactant protein d. *Front Immunol* (2018) 9:1586. doi: 10.3389/fimmu.2018.01586
44. LeVine AM, Whitsett JA, Hartshorn KL, Crouch EC, Korfhagen TR. Surfactant protein d enhances clearance of influenza a virus from the lung in vivo. *J Immunol* (2001) 167(10):5868–73. doi: 10.4049/jimmunol.167.10.5868
45. Pandit H, Gopal S, Sonawani A, Yadav AK, Qaseem AS, Warke H, et al. Surfactant protein d inhibits HIV-1 infection of target cells via interference with Gp120-CD4 interaction and modulates pro-inflammatory cytokine production. *PLoS One* (2014) 9(7):e102395. doi: 10.1371/journal.pone.0102395
46. Pandit H, Kale K, Yamamoto H, Thakur G, Rokade S, Chakraborty P, et al. Surfactant protein d reverses the gene signature of transepithelial HIV-1 passage and restricts the viral transfer across the vaginal barrier. *Front Immunol* (2019) 10:264. doi: 10.3389/fimmu.2019.00264
47. Amraei R, Yin W, Napoleon MA, Suder EL, Berrigan J, Zhao Q, et al. CD209L/L-SIGN and CD209/DC-SIGN act as receptors for SARS-CoV-2. *ACS Cent Sci* (2021) 7(7):1156–65. doi: 10.1021/acscentsci.0c01537
48. Lempp FA, Soriaga LB, Montiel-Ruiz M, Benigni F, Noack J, Park Y-J, et al. Lectins enhance SARS-CoV-2 infection and influence neutralizing antibodies. *Nature* (2021) 598(7880):342–7. doi: 10.1038/s41586-021-03925-1
49. Jin C, Wu L, Li J, Fang M, Cheng L, Wu N. Multiple signaling pathways are involved in the interleukin-4 regulated expression of DC-SIGN in THP-1 cell line. *J Biomedicine Biotechnol* (2012) 2012:357060. doi: 10.1155/2012/357060
50. Abraham MJ, Murtola T, Schulz R, Páll S, Smith JC, Hess B, et al. GROMACS: High performance molecular simulations through multi-level parallelism from laptops to supercomputers. *SoftwareX* (2015) 1-2:19–25. doi: 10.1016/j.softx.2015.06.001
51. Lindorff-Larsen K, Piana S, Palmo K, Maragakis P, Klepeis JL, Dror RO, et al. Improved side-chain torsion potentials for the amber Ff99sb protein force field. *Proteins* (2010) 78(8):1950–8. doi: 10.1002/prot.22711
52. Mogensen TH. Pathogen recognition and inflammatory signaling in innate immune defenses. *Clin Microbiol Rev* (2009) 22(2):240–73. doi: 10.1128/CMR.00046-08
53. Li D, Wu M. Pattern recognition receptors in health and diseases. *Signal Transduct Targeted Ther* (2021) 6(1):1–24. doi: 10.1038/s41392-021-00687-0
54. Lai C-C, Shih T-P, Ko W-C, Tang H-J, Hsueh P-R. Severe acute respiratory syndrome coronavirus 2 (SARS-CoV-2) and coronavirus disease-2019 (COVID-19): The epidemic and the challenges. *Int J Antimicrob Agents* (2020) 55(3):105924. doi: 10.1016/j.ijantimicag.2020.105924
55. Hu B, Guo H, Zhou P, Shi Z-L. Characteristics of SARS-CoV-2 and COVID-19. *Nat Rev Microbiol* (2021) 19(3):141–54. doi: 10.1038/s41579-020-00459-7
56. Xu J, Xu X, Jiang L, Dua K, Hansbro PM, Liu G. SARS-CoV-2 induces transcriptional signatures in human lung epithelial cells that promote lung fibrosis. *Respir Res* (2020) 21(1):1–12. doi: 10.1186/s12931-020-01445-6
57. Perrotta F, Matera MG, Cazzola M, Bianco A. Severe respiratory SARS-CoV2 infection: Does ACE2 receptor matter? *Respir Med* (2020) 168:105996. doi: 10.1016/j.rmed.2020.105996
58. Marzi A, Möller P, Hanna SL, Harrer T, Eisemann J, Steinkasserer A, et al. Analysis of the interaction of Ebola virus glycoprotein with DC-SIGN (Dendritic cell-specific intercellular adhesion molecule 3–grabbing nonintegrin) and its homologue DC-SIGNR. *J Infect Dis* (2007) 196(Supplement\_2):S237–46. doi: 10.1086/520607
59. Pöhlmann S, Leslie GJ, Edwards TG, Macfarlan T, Reeves JD, Hiebenthal-Millow K, et al. DC-SIGN interactions with human immunodeficiency virus: Virus binding and transfer are dissociable functions. *J Virol* (2001) 75(21):10523–6. doi: 10.1128/JVI.75.21.10523-10526.2001
60. Benton DJ, Wrobel AG, Xu P, Roustan C, Martin SR, Rosenthal PB, et al. Receptor binding and priming of the spike protein of SARS-CoV-2 for membrane fusion. *Nature* (2020) 588(7837):327–30. doi: 10.1038/s41586-020-2772-0
61. Shang J, Ye G, Shi K, Wan Y, Luo C, Aihara H, et al. Structural basis of receptor recognition by SARS-CoV-2. *Nature* (2020) 581(7807):221–4. doi: 10.1038/s41586-020-2179-y
62. Murgolo N, Therien AG, Howell B, Klein D, Koeplinger K, Lieberman LA, et al. SARS-CoV-2 tropism, entry, replication, and propagation: Considerations for drug discovery and development. *PLoS Pathog* (2021) 17(2):e1009225. doi: 10.1371/journal.ppat.1009225
63. Liu J, Zhang X, Cheng Y, Cao X. Dendritic cell migration in inflammation and immunity. *Cell Mol Immunol* (2021) 18(11):2461–71. doi: 10.1038/s41423-021-00726-4
64. Marongiu L, Valache M, Facchini FA, Granucci F. How dendritic cells sense and respond to viral infections. *Clin Sci* (2021) 135(19):2217–42. doi: 10.1042/CS20210577
65. Farahani M, Niknam Z, Amirabad LM, Amiri-Dashatan N, Koushki M, Nemati M, et al. Molecular pathways involved in COVID-19 and potential pathway-based therapeutic targets. *Biomed Pharmacother* (2022) 145:112420. doi: 10.1016/j.biopha.2021.112420
66. Yang L, Xie X, Tu Z, Fu J, Xu D, Zhou Y. The signal pathways and treatment of cytokine storm in COVID-19. *Signal Transduct Targeted Ther* (2021) 6(1):1–20. doi: 10.1038/s41392-021-00679-0
67. Mogensen TH, Paludan SR. Molecular pathways in virus-induced cytokine production. *Microbiol Mol Biol Rev* (2001) 65(1):131–50. doi: 10.1128/MMBR.65.1.131-150.2001
68. Kircheis R, Haasbach E, Lueftenecker D, Heyken WT, Ocker M, Planz O. NF- $\kappa$ B pathway as a potential target for treatment of critical stage COVID-19 patients. *Front Immunol* (2020) 11:3446. doi: 10.3389/fimmu.2020.598444
69. Hirano T, Murakami M. COVID-19: A new virus, but a familiar receptor and cytokine release syndrome. *Immunity* (2020) 52(5):731–3. doi: 10.1016/j.immuni.2020.04.003
70. Kircheis R, Haasbach E, Lueftenecker D, Heyken WT, Ocker M, Planz O. Perspective: NF- $\kappa$ B pathway as a potential target for treatment of critical stage COVID-19 patients. (2020) 11:598444. doi: 10.3389/fimmu.2020.598444
71. Barhoumi T, Alghanem B, Shaibah H, Mansour FA, Alamri HS, Akiel MA, et al. SARS-CoV-2 coronavirus spike protein-induced apoptosis, inflammatory, and oxidative stress responses in THP-1-Like-Macrophages: Potential role of angiotensin-converting enzyme inhibitor (Perindopril). *Front Immunol* (2021) 12. doi: 10.3389/fimmu.2021.728896
72. Mukhopadhyay S, Hoidal JR, Mukherjee TK. Role of tnf $\alpha$  in pulmonary pathophysiology. *Respir Res* (2006) 7(1):1–9. doi: 10.1186/1465-9921-7-125
73. Muñoz-Carrillo JL, Contreras-Cordero JF, Gutiérrez-Coronado O, Villalobos-Gutiérrez PT, Ramos-Gracia LG, Hernández-Reyes VE. Cytokine profiling plays a crucial role in activating immune system to clear infectious pathogens. In: *Immune response activation and immunomodulation*. IntechOpen (2018) 2019. doi: 10.5772/intechopen.80843
74. Chen G, Wu D, Guo W, Cao Y, Huang D, Wang H, et al. Clinical and immunological features of severe and moderate coronavirus disease 2019. *J Clin Invest* (2020) 130(5):2620–9. doi: 10.1172/JCI137244
75. Huang C, Wang Y, Li X, Ren L, Zhao J, Hu Y, et al. Clinical features of patients infected with 2019 novel coronavirus in wuhan, China. *Lancet* (2020) 395(10223):497–506. doi: 10.1016/S0140-6736(20)30183-5
76. Qin C, Zhou L, Hu Z, Zhang S, Yang S, Tao Y, et al. Dysregulation of immune response in patients with COVID-19 in wuhan, china; clinical infectious diseases; Oxford academic. *Clin Infect Dis* (2020) 28;71(15):762–8. doi: 10.1093/cid/cia248
77. Makwana R, Gozzard N, Spina D, Page C. TNF- $\alpha$ -Induces airway hyperresponsiveness to cholinergic stimulation in Guinea pig airways. *Br J Pharmacol* (2012) 165(6):1978–91. doi: 10.1111/j.1476-5381.2011.01675.x
78. Peiris J, Lai S, Poon L, Guan Y, Yam L, Lim W, et al. Coronavirus as a possible cause of severe acute respiratory syndrome. *Lancet* (2003) 361(9366):1319–25. doi: 10.1016/S0140-6736(03)13077-2
79. Chen I-Y, Moriyama M, Chang M-F, Ichinohe T. Severe acute respiratory syndrome coronavirus viroporin 3a activates the NLRP3 inflammasome. *Front Microbiol* (2019) 10:50. doi: 10.3389/fmicb.2019.00050
80. Warke T, Fitch P, Brown V, Taylor R, Lyons J, Ennis M, et al. Exhaled nitric oxide correlates with airway eosinophils in childhood asthma. *Thorax* (2002) 57(5):383–7. doi: 10.1136/thorax.57.5.383

81. Wang X, Jiang W, Yan Y, Gong T, Han J, Tian Z, et al. RNA Viruses promote activation of the NLRP3 inflammasome through a RIP1-RIP3-DRP1 signaling pathway. *Nat Immunol* (2014) 15(12):1126–33. doi: 10.1038/ni.3015
82. Jones SA, Jenkins BJ. Recent insights into targeting the IL-6 cytokine family in inflammatory diseases and cancer. *Nat Rev Immunol* (2018) 18(12):773–89. doi: 10.1038/s41577-018-0066-7
83. Tanaka T, Narazaki M, Kishimoto T. IL-6 in inflammation, immunity, and disease. *Cold Spring Harbor Perspect Biol* (2014) 6(10):a016295. doi: 10.1101/cshperspect.a016295
84. Chen X, Zhao B, Qu Y, Chen Y, Xiong J, Feng Y, et al. Detectable serum SARS-CoV-2 viral load (RNAemia) is closely correlated with drastically elevated interleukin 6 (IL-6) level in critically ill COVID-19 patients. *Clin Infect Dis* (2020) 71(8):1937–42. doi: 10.1093/cid/ciaa449
85. Herold T, Jurinovic V, Arnreich C, Lipworth BJ, Hellmuth JC, von Bergwelt-Baildon M, et al. Elevated levels of IL-6 and CRP predict the need for mechanical ventilation in COVID-19. *J Allergy Clin Immunol* (2020) 146(1):128–136. e4. doi: 10.1016/j.jaci.2020.05.008
86. Lee AJ, Ashkar AA. The dual nature of type I and type II interferons. *Front Immunol* (2018), 11, 9:2061. doi: 10.3389/fimmu.2018.02061
87. Hargadon KM, Zhou H, Albrecht RA, Dodd HA, Garcia-Sastre A, Braciale TJ. Major histocompatibility complex class II expression and hemagglutinin subtype influence the infectivity of type A influenza virus for respiratory dendritic cells. *J Virol* (2011) 85(22):11955–63. doi: 10.1128/JVI.05830-11
88. Braciale TJ, Sun J, Kim TS. Regulating the adaptive immune response to respiratory virus infection. *Nat Rev Immunol* (2012) 12(4):295–305. doi: 10.1038/nri3166
89. Toulmin SA, Bhadiadra C, Paris AJ, Lin JH, Katzen J, Basil MC, et al. Type II alveolar cell MHCII improves respiratory viral disease outcomes while exhibiting limited antigen presentation. *Nat Commun* (2021) 12(1):1–15. doi: 10.1038/s41467-021-23619-6
90. Sokol CL, Luster AD. The chemokine system in innate immunity. *Cold Spring Harbor Perspect Biol* (2015) 7(5):a016303. doi: 10.1101/cshperspect.a016303
91. Kobayashi Y. The role of chemokines in neutrophil biology. *Front Biosci* (2008) 13(1):2400–7. doi: 10.2741/2853
92. Zuo Y, Yalavarthi S, Shi H, Gockman K, Zuo M, Madison JA, et al. Neutrophil extracellular traps in COVID-19. *JCI Insight* (2020) 5(11):e138999. doi: 10.1172/jci.insight.138999
93. Posch W, Vosper J, Noureen A, Zaderer V, Witting C, Bertacchi G, et al. C5aR inhibition of nonimmune cells suppresses inflammation and maintains epithelial integrity in SARS-CoV-2-infected primary human airway epithelia. *J Allergy Clin Immunol* (2021) 147(6):2083–97.e6. doi: 10.1016/j.jaci.2021.03.038
94. Patterson BK, Seethamraju H, Dhody K, Corley MJ, Kazempour K, Lalezari J, et al. Disruption of the CCL5/RANTES-CCR5 pathway restores immune homeostasis and reduces plasma viral load in critical COVID-19. *MedRxiv* (2020) 5:2020.05.02.20084673. doi: 10.1101/2020.05.02.20084673